A SURVEY AND COMPARISON OF VARIOUS OPTICAL PERFORMANCE METRICS

By

Mark R. Burgener

A Master's Report Submitted to the Faculty of the

COLLEGE OF OPTICAL SCIENCE

In Partial Fulfillment of the Requirements

For the Degree of

MASTER OF SCIENCE

In the Graduate College

THE UNIVERSITY OF ARIZONA

2021

Thesis Committee Approval Page

ACKNOWLEDGMENTS

I would like to thank the faculty and distance staff of the College of Optical Sciences. It has been excellent and at times challenging learning experience. I have learned a lot over this education journey and feel better prepared to continue my work in the field. I would like to thank the chair of my Master's Committee, Professor Jim Schwiegerling, as well as the members of the Master's Committee, Professor Matthew Kupinski and Professor Rongguang Liang.

I would also like to thank all of the people that I work with that have supported me; financially, expertise, and patience; though my time pursuing this education. Finally, I would like to thank my family for the encouragement to succeed.

Table of Contents

LIST OF FIGURES

LIST OF TABLES

ABSTRACT

Development of optical systems always starts with high level requirements and is then reduced down to system and then to component requirements, such as Modulation Transfer Function, Field of View, Resolution, and F-Number to name a few. In many cases the highest level requirement from a customer comes in terms of performance requirements. Through the use of modeling and simulation against range performance allows an optical engineer to predict the performance of the component and system requirements they have developed to meet these higher level customer requirements. Decades of research has gone into the modeling and simulation of human performance viewing imaging system outputs and have resulted in various metric for use in this type of modeling and simulation. The following report explores the definition and ultimately a comparison of some of these various metrics. Based on the theory of these metrics six sensors were modeled; three infrared and three visible; using the Night-Vision Integrated Performance Model. The results of the different metrics were compared and a recommendation for which metrics to utilize was provided based on the metric limitations and results.

1 Introduction

In the study and application of optical science and optical design the main goal is to develop or design a system meeting certain design criteria, while providing the best optical system within the required design constraints. Design constrains usually consist of cost, quality, manufacturability, time to produce, and for some customers durability. This paper is going to be focusing on quality metrics. During the study and application of optical science, a primary focus is placed on optical design quality metrics. Figures 1(a-e) and show an example some of the standard diagrams an optical designer looks at during the design phase of an optical system. Spot Diagrams that point to if the system is resolution or optics limited, Figure 1(a). Field Curvature, Distortion, Optical Path Difference (OPD) plots, and Seidel Diagrams that show what kind and how much of a given aberration will be present in an optical design, Figures 1(b, c, e). The Modulation Transfer Function (MTF) shows the amount of attenuation, or blur produced by various parts of an optical or imaging system, Figure 1(d), with Figure 2 demonstrating an example of MTF effects to a target of a given spatial resolution.

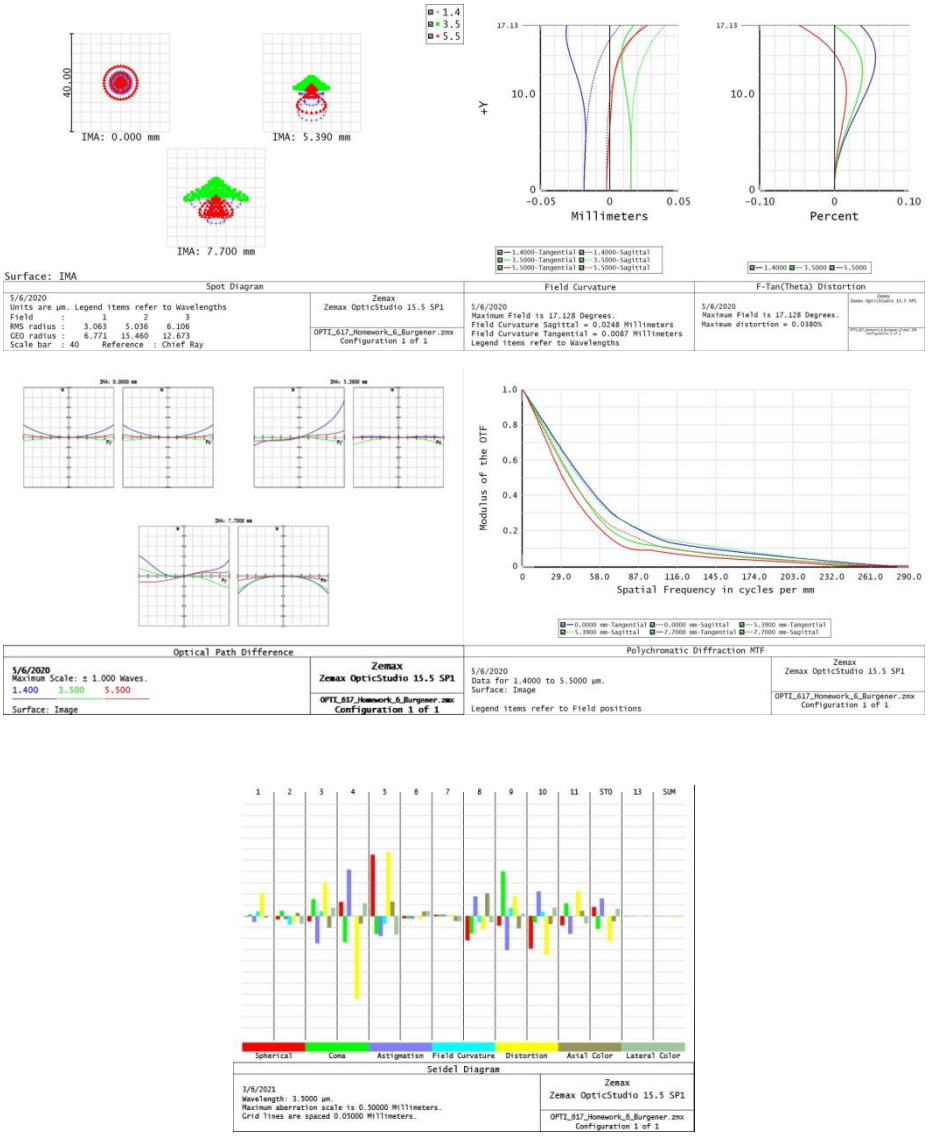

Figure 1: Zemax Outputs [1]

(a) Spot Diagrams, (b) Field Curvature Diagram), (c) OPD Diagram, (d) MTF Diagram, (e) Seidel Diagram

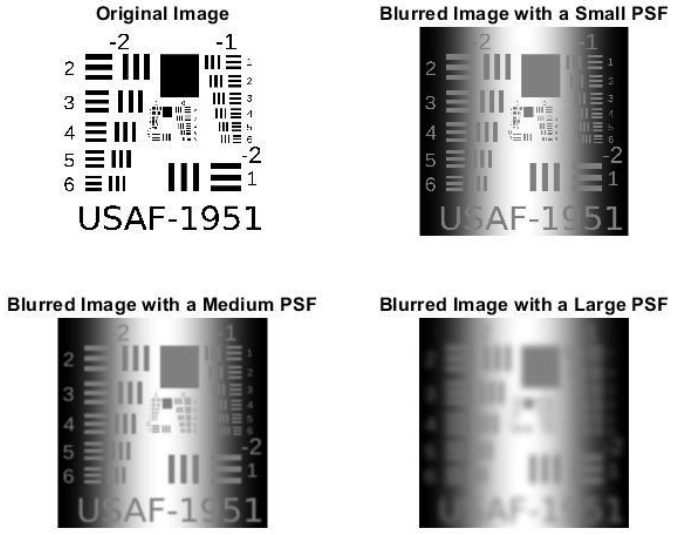

Figure 2: MTF Effects Example [2]

[Modified using included MATLAB script]

There are a few others that are commonly used, such as Encircled or Ensquared Energy, Root Mean Squared (RMS) Wavefront Error, Point Spread Function (PSF), and Strehl Ratio to name a few. However, these optical design metrics or quality factors are normally the result of the flow down of requirements of the imaging system. The end user will usually have imaging performance requirements as the ultimate high level requirement. An end user may say their requirement is to Identify a Ford™ truck at 500 meters, or they need to Detect a specific type and size of tumor, or they need to Recognize a tank at 2,000 meters. Each of these tasks; Detection, Recognition, and Identification; require a prediction capability that is tasked based, that will assess if the end requirement is ultimately satisfied by an optical system design. There are a few task based performance metrics that will be surveyed in this report; Johnson Criteria, Thermal Range Model 4, National Imagery Interpretation Rating System, and the Target Task Performance Metric. Each of these has a use and will be discussed in detail, but ultimately they attempt to put metrics on what probability a human can perceive or perform the given task. The focus of the metric comparison will be on broadband imaging systems assuming a far field imaging requirement.

2 Performance Metrics

2.1 Johnson Criteria

Johnson Criteria was originally developed by John Johnson and published in 1958. Johnson's study did two things. The first was to create four levels of discrimination; Detection, Orientation, Recognition, and Identification [3]. Table 1 provides the definitions for each level of discrimination, or target discrimination tasks. Over the years since Johnson published there have been expansions and revisions to the original discrimination level lists; however the standard three, Detection, Recognition, and Identification are still commonly used in the system performance modeling field.

Table 1: Johnson Criteria

(From [3 and 4])

Discrimination Level	Meaning
Detection	The object has a reasonable probability of being an object being sought
Orientation	The objects orientation may be discerned
Recognition	Object resolved with sufficient clarity that its specific class could be differentiated
Identification	Object resolved with sufficient clarity to specify the type within the class

Johnson's original goal was to develop a way to relate real world targets which have significantly different shapes, contrasts, and can be viewed at varying ranges, to a standard methodology of simplified targets. Johnson selected square wave patterns. Johnson would vary the range of the targets of interest of his original study until the task (Detection, Orientation, Recognition, or Identification) could just be performed and would then insert a spatial frequency chart (bar-chart; example shown in Figure 3) into the Field of View (FOV) and vary the spatial frequency until the observer was just able to resolve the bar chart [4].

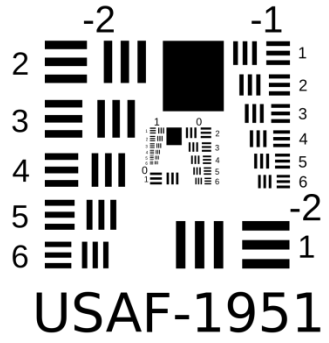

Figure 3: United States Air Force (USAF) 1951 Resolution Chart [2]

This approach was repeated with various observers to attempt to characterize "the average observer" [6]. The Johnson paper produced minimum resolution requirements in order to perform each task in terms of the number of cycles required to perform each task. A cycle is the size of a black and white bar, see Figure 3 as reference. Since Johnson performed his experiments at the point of Just Noticeable Difference (JND) the cycle criterion that was generated represented the 50% level of discrimination. This became known as the N_{50} value, or the number of cycles required to perform the task for 50% performance. The original set of N_{50} values as defined by Johnson are provided in Table 2.

Table 2: Johnson Criteria N_{50} Values

(From [4])

Discrimination Level	N_{50}
Detection	1.0
Orientation	1.4
Recognition	4.0
Identification	6.4

From this information the 1975 Night Vision Lab (NVL) modeling program derived Equations 1 and 2 to define the performance of a given task (Detection, Orientation, Recognition, or Identification), where the Probability of Task performance or P(Task) is the probability that the observer can complete the task, N_{50} is the Johnson Criteria provided in Table 2, and N is the actual number of cycles across the target at a given range.

$$P(Task) = \frac{\left(N/N_{50}\right)^E}{1+\left(N/N_{50}\right)^E}$$ Equation 1 [3 and 5]

$$E = 2.7 + 0.7 * \left(\frac{N}{N_{50}}\right)$$ Equation 2 [3 and 5]

When Equations 1 and 2 are applied to varying N values it can be seen in Figure 4 that with a lower N_{50} value the probability of completing the task approaches 100% fast than those with higher N_{50} values. This shows that, and as logic dictates based on Table 2, with understanding that the N_{50} is cycle criteria or spatial frequencies on a bar-chart that the lower the N_{50} value the "easier" the task is for the observer to complete.

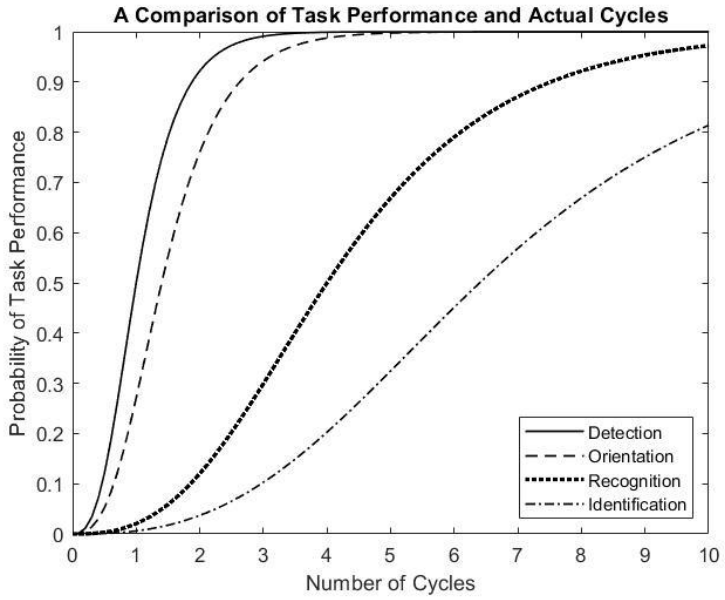

Figure 4: Probability vs. N

In Johnson's experiments he used the targets minimum dimension meaning that the 1975 NVL model utilized a one dimensional assumption. This was later revised during the development of two dimensional programs, such as FLIR92, NVTherm, and subsequent performance modeling programs. During this adjustment it was realized that the target size was now dependent on viewing angle and was altered to use the square root of the target area [3]. During the research into these alternations to the assumptions

it was also found that the N_{50} values, due to this target aspect dependence and the P(Task)'s also had to change, due to a differentiation between and a casual and highly motivated observer [3]. Table 3 shows the two dimension N_{50} criteria, Equations 3 and 4 show the updated P(Task) and E_j expressions for the two dimensional for the performance predictions, and Figure 5 shows the updated probability vs. N curves based on Equations 3 and 4. Reviewing Figure 5 shows that the same relationships between N_{50} and task difficulty is similar to Figure 4, but shows a greater separation between Detection and Orientation or the newly defined Classification term. Classification is defined as "The broad class of object types to which the object belongs may be determined" [3, 4]. This is a result of a different definition in Classification versus Orientation which results in a minor difference in the N_{50} value, but also with the new N_{50} for Detection also resulting in a reduced value for the two dimensional Johnson Criteria.

Table 3: 2D Johnson Criteria N_{50} Values

(From [3, 4, 5])

Discrimination Level	N_{50}
Detection	0.75
Classification	1.5
Recognition	3.0
Identification	6.0

$$P(Task) = \frac{\left(N/N_{50}\right)^{E_j}}{1+\left(N/N_{50}\right)^{E_j}} \qquad \text{Equation 3 [6]}$$

$$E_J = 1.75 + 0.35 * \left(\frac{N}{N_{50}}\right) \qquad \text{Equation 4 [6]}$$

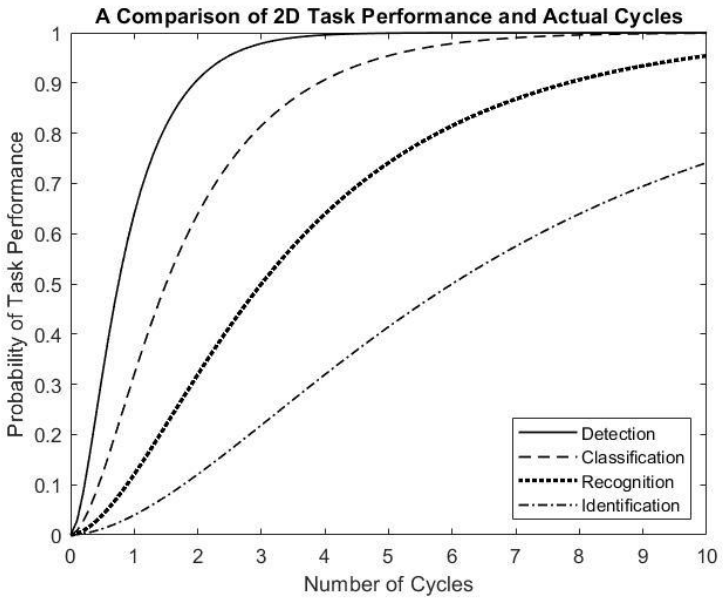

Figure 5: 2D Probability vs. N

To help with a comparison of the one dimensional versus the two dimensional P(Task) equations they were replotted by task (Detection, Orientation / Classification, Recognition, and Identification). For the purposes of an accurate comparison, the Orientation / Classification are included but are not going to be discussed, due to the change in definitions from the one dimensional experiments to the two dimensional. The other three standard terms do not change much and can thus, be fairly compared. As can be seen in Figure 6(a, c, d), at lower spatial frequencies (N) the two dimensional curve results in a higher probability of task completion. However, in all the plots at a given high spatial frequency the two plots cross leading to the assumption that at low spatial frequencies the one dimensional under predicts performance while at high spatial frequencies it over predicts in comparison to the two dimensional calculations.

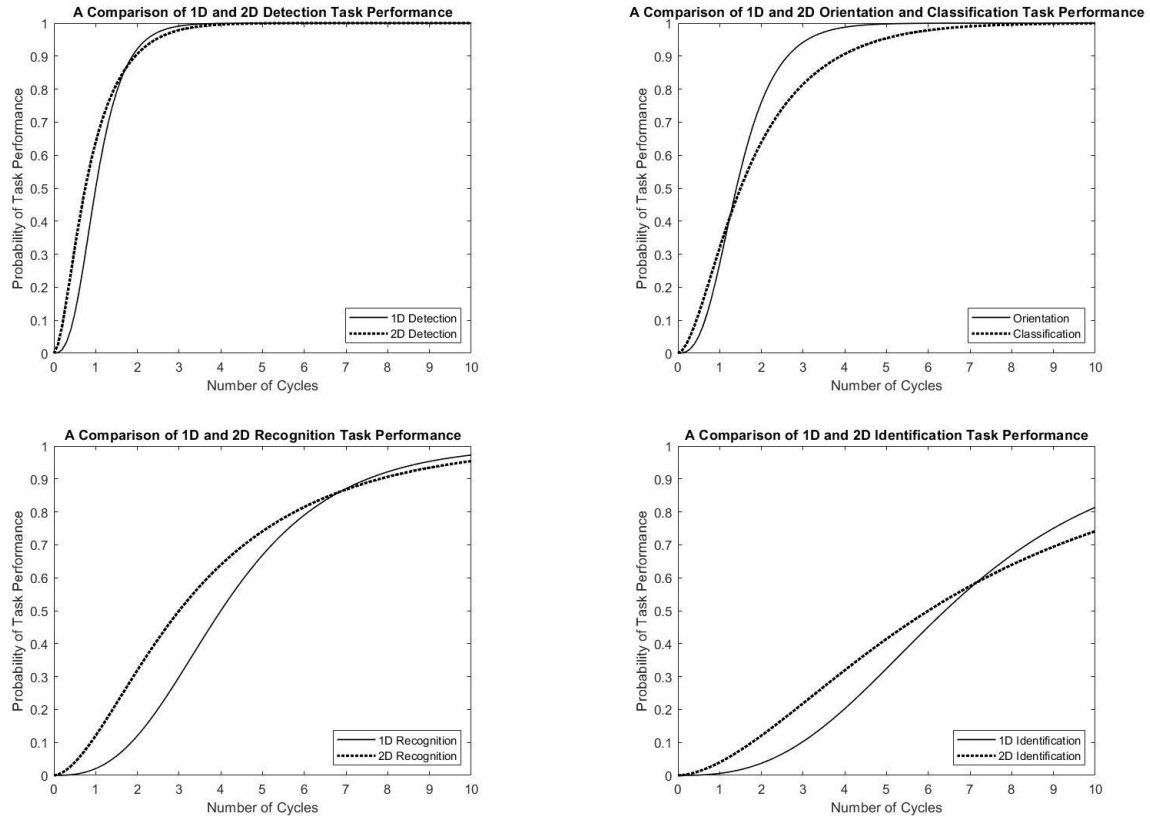

Figure 6: 2D Task Comparison of Probability vs. N

(a) Detection, (b) Orientation / Classification, (c) Recognition, (d) Identification

Originally Johnson Criteria was developed for direct view imaging systems. The use of the two dimensional criteria was later expanded and validated for use with digital systems, such as infrared systems [3]. These new expansions and validations were used in the development of the follow on performance models from the 1975 NVL model, FLIR92 and NVTherm.

The method to convert the P(Task) values into range performance required the systems Minimum Resolvable Temperature (MRT) or Minimum Resolvable Contrast (MRC) curves as a function of spatial frequency. Essentially at each range the effective target temperature was calculated and was referenced to the corresponding frequency on the MRC measurements or predictions. This frequency was then multiplied by the target angular subtense, which results in the N value that would then be applied to the

Equations 3 and 4 which would give a probability value for the given range as shown in Equations 5 and 6.

$$N = \alpha * f \qquad \text{Equation 5 [9]}$$

$$N = f * \frac{h_c}{R} \qquad \text{Equation 6 [3, 9]}$$

Where;

$\alpha = Angular\ subtense$

$f = Spatial\ frequency$

$R = Range$

$h_c = Target's\ Charateristic\ Dimension$

This process would then be repeated for all range values required [3, 4]. Since MRTs and MRCs are measured values which can only be accurately taken after the system is built there was another approach that was taken when applying Johnson Criteria to system performance predictions. In the modeling phase MRT is replaced in the equation with the Contrast Threshold Function (CTF) of the modeled system. Therefore the N term given a range is selected by the intersection of the apparent target contrast and the CTF. An example of this approach is shown in Figure 7. This gives the spatial frequency that is than applied to the calculation described above [7].

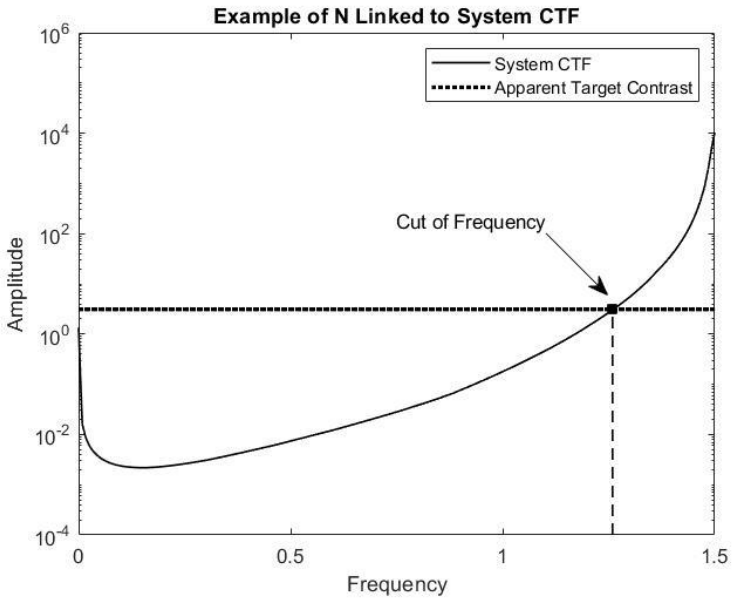

Figure 7: Example System CTF versus Apparent Target Contrast

There is another approach that is commonly used that references Johnson Criteria, and that is the association on pixels on target as metric for defining performance. Various texts use the cycle criteria, which is defined as one black bar and one white bar on a resolution test chart (see Figure 2 for reference), to equate cycle criteria to two pixels of an imager, or the size of two Instantaneous Fields of Views (IFOVs) projected at range. Equations 7 and 8 define this methodology [6].

$$\xi = \frac{n_{cycles}}{x/_R} = \frac{1}{2*IFOV} = \frac{f}{2*\sqrt{A}} \qquad \text{Equation 7}$$

$$\xi = \frac{2*R*N_{50}}{x} \qquad \text{Equation 8}$$

Where;

$x = Minimum\ target\ dimension, or\ square\ root\ of\ the\ target\ area$

$R = Range$

$A = Area\ of\ the\ detector$

The method seems like a very attractive approach to do a back of the envelop calculation. However, as can be seen in Equations 7 and 8, there is no reference to

target contrast either through MRT/MRC or CTF, or any losses related to atmospherics; such as absorption, or blur. This assumes that the system is resolution limited and not noise or contrast limited. The comparison of this approach to range predictions based on modeled Johnson Criteria will be addressed in a later section.

This issue with Johnson Criteria can be seen in the deeper calculations discussed above. It fundamentally assumes, through the use of MRT and MRC, two things. The first is that the system is always dominated by Signal to Noise Ratio (SNR), or contrast of the target, and the limiting factor is resolution. With the direct view systems that Johnson was originally measuring, or in early digital systems where the bit depth and dynamic range were low and the system resolutions was small compared to today's modern imagers, this was a valid assumption. As imager technology progressed into higher resolution, smaller pixel pitches, better bit depth, and higher dynamic range sensors this caused a transition from the Johnson assumptions about being resolution limited, to assumptions that systems were more noise and contrast limited thus, causing the fundamental relation of spatial frequency alone to be inaccurate for modern imaging systems.

The second issue with Johnson as described above is that the system description of performance is tied to the MRTs or MRCs of the system. These values are only really accurately obtained through lab measurements, which mean that the system must first be built prior to modeling performance. The early iterations of the models built off of Johnson Criteria such as 1975 NVL, FLIR92, and NVTherm, provided methods to predict MRTs to help with this issue; however it was always documented that it could not be used to predict lab measurements, which led to less accurate modeled performance prior to testing the system [3, 4].

2.2 National Imagery Interpretation Rating System (NIIRS)

The next metric that is going to be covered is the National Imagery Interpretation Rating System or NIIRS. The NIIRS metric came into existence in the 1970s as the 10 point Imagery Interpretability Rating Scale (IIRS) and then was updated in the 1994 to become NIIRS [3]. Unlike the Johnson Criteria NIIRS was developed as an

interpretability rating system for imagery, originally film, captured from air platforms [3, 8, 9, 10, 11]. The intent of IIRS was to relate Ground Resolved Distance (GRD) to a rating system developed with criteria considered for intelligence purposes [3]. The development of the NIIRS metric was done to transition away from IIRS metric "arose from the inability of simple physical image quality measures, such as resolution, to adequately predict image interpretability" [8].

There are currently 6 NIIRS rating scales that have been published. They are Visible, Civil, Radar, Infrared, Multispectral, and Video [8, 11]. For the purposes of this paper the focus is going to be on the Visible and Infrared versions of NIIRS. The Radar NIIRS does not apply to the purpose of this paper, and the model that will be used to compare these metrics, the Night Vision – Integrated Performance Model (NV-IPM), only can handle the Visible and Infrared versions of the calculations. Table 8 in Appendix B shows excerpts from several references that define the Visible, Infrared, Civil, and Video NIIRS ratings systems. All of the static NIIRS ratings systems are on a 0 to 9 scale of image interpretability. Each NIIRS rating contains; a discrimination level, such as Detection or Identification; an object, such as a ship or vehicle registration numbers; and a modifier, such as in port or on a truck [3].

The exception to that is the Video NIIRS (V-NIIRS) rating system that starts at a V-NIIRS of 3 "because resolvable items at these gross resolutions are generally too large to move at a speed that requires motion imagery" [11]. In addition to the discrimination level, object, and modifier, V-NIIRS also added an action modifier to its criteria to account for the nature of motion in a clip of video. NIIRS and other metrics such as Johnson and the Target Task Performance Metric (TTPM) do not limit the time to make a discrimination task call from an observer, nor do they typically use motion in its criteria unless specifically referenced in the development study for a TTPM value. V-NIIRS attempted to use motion as an indicator based on technology advances, i.e. transition from still imagery to motion imagery applications for air platforms [11].

As can be seen in Table 8 in Appendix B, the NIIRS scale definitions can be interpreted as being subjective [3]. However, in the 1980s the General Image Quality

Equation (GIQE) was developed and released to the public in 1994 when NIIRS was updated to the current rating scales [12]. With the GIQE, NIIRS can now be calculated using system information [3, 10]. Equation 9 shows the original version of the GIQE. The original version of the GIQE uses $_{GM}$ modifiers to represent the geometric mean of the horizontal and vertical values for Relative Edge Response (RER) and Ground Sample Distance (GSD) values [10].

$$NIIRS = 11.81 + 3.32 * log_{10}\left(\frac{RER_{GM}}{GSD_{GM}}\right) - 1.48 * H_{GM} - \left(\frac{G}{SNR}\right) \quad \text{Equation 9 [10]}$$

There are a couple of other equations or functions referenced in Equations 9. The first is the RER_{GM} function that is shown in Equation 10, which requires the Edge Response (ER) of the system using the measured or predicted system MTF detailed in Equations 11 and 12. The RER_{GM} uses the Edge Reponses at the +0.5 and -0.5 pixels from the edge in each direction.

$$RER_{GM} = \sqrt{[ER_x(0.5) - ER_x(-0.5)] * [ER_y(0.5) - ER_y(-0.5)]} \quad \text{Equation 10 [10]}$$

$$ER_x = 0.5 + \frac{1}{\pi}\int_0^\infty \frac{MTF_x(\xi)}{\xi} * sin(2 * \pi * x * \xi)d\xi \quad \text{Equation 11 [10]}$$

$$ER_y = 0.5 + \frac{1}{\pi}\int_0^\infty \frac{MTF_y(\xi)}{\xi} * sin(2 * \pi * y * \xi)d\xi \quad \text{Equation 12 [10]}$$

The second is the GSD function that is show in Equations 13 and 14. The third is the overshoot due to edge sharpening (H) function is defined by the maximum Edge Response (ER) of pixels 1 to 3 from the edge in Equations 11 and 12. The fourth is the noise gain produced by edge sharpening (G), which is defined by Equation 15 and represents the Modulation Transfer Function (MTF) Compression or Edge Sharpening. This is determined by a kernel in an M x N matrix. The fifth is the Signal to Noise (SNR) of the system, which is measured or modeled value, of the differential scene radiance to the system RMS noise [10].

$$GSD_x = \frac{d_x}{f} * R$$ Equation 13 [10]

$$GSD_y = \frac{d_y}{f} * R$$ Equation 14 [10]

$$G = \sqrt{\sum_{i=1}^{M} \sum_{j=1}^{N} \left(Kernel_{ij}\right)^2}$$ Equation 15 [10]

While these values represent the original version of the GIQE there have been some updates to GIQE with version 4 [3]. In addition GSD values, Equations 13 and 14, assumes the imaging system in always looking Nadir, or directly down. The following equations are the updates from version 4 of NIIRS and the implementation within the NV-IPM software to allow for variations across NIIRS spectral bands and changes in GSD as a function of slant range. Equation 16 is the first item to change. It applies a variable C value depending on if the modeler is selecting Visible or Infrared NIIRS predictions.

$$NIIRS = C + a * log_{10}\left(GSD_g\right) + b * log_{10}(RER) - 0.656 * H - 0.344 * \left(\frac{G}{SNR}\right)$$ Equation 16 [12]

Where;

$C_{Thermal} = 10.751$ or $C_{Visible} = 10.251$ [12]

When;

$RER \geq 0.9$ [3, 12]

$a = 3.32$ and $b = 1.559$ [3, 12]

When;

$RER < 0.9$ [3, 12]

$a = 3.16$ and $b = 2.817$ [3, 12]

One of the primary outputs of the NV-IPM software is probability of task performance or NIIRS rating as a function of range. The original GIQE assumes that the range (R) is always equal to the altitude of the aircraft, i.e. Nadir viewing angle. NV-IPM assumes a fixed target, or sensor altitude so as the GIQE equation is varies over range with a fixed sensor or target altitude the GSD of the sensor is going have an angular component. NV-IPM added edits to the GSD equations shown in Equations 17 and 18 to account for line of sight view angle relative to the horizon, i.e. downlook angle 0° being Nadir and 90° being horizontal slant path. Just like the original GIQE, NV-IPM uses the geometric mean of the GSD, found in Equation 19.

$$\mathrm{GSD_x} = \frac{\mathrm{d_x}}{\mathrm{f}} * \frac{\mathrm{R}}{\cos\theta} \qquad \text{Equation 17 [12]}$$

$$\mathrm{GSD_y} = \frac{\mathrm{d_y}}{\mathrm{f}} * \frac{\mathrm{R}}{\cos\theta} \qquad \text{Equation 18 [12]}$$

$$\mathrm{GSD_g} = \sqrt{\mathrm{GSD_x} * \mathrm{GSD_y}} \qquad \text{Equation 19 [12]}$$

NV-IPM uses the same RER_{GM}, ER_x, and ER_y calculations as Equations 10, 11 and 12. It also calculates the H value in a similar manner using pixels from 1 to 3 from the edge, but uses increments of 0.25 pixels, however “If the value of the edge response monotonically increases over this range than the overshoot is the value of the edge response at 1.25 pixels.” [12]. The last difference in the GIQE from the original to what is applied in the NV-IPM software is the G value. Since NV-IPM allows for the application of several different post-processing components in a given system and most common systems today use many post-processing image enhancement algorithms. NV-IPM used Parseval’s theorem to find G, Equation 20. Equation 20 uses the post sampled MTF input or predictions [12].

$$\mathrm{G} = 2 * \int_0^1 \mathrm{MTF_{Post}}(\xi)^2 \mathrm{d}\xi \qquad \text{Equation 20 [12]}$$

The last topic that is going to be needed for when the various metrics are compared is a relationship to NIIRS and another metric. For that, Equation 21 relates the N values from Johnson Criteria and the size of the target to a GSD value.

$$N_{Cycles} = \frac{h_c}{2*GSD} \quad \text{Equation 21 [3, 9]}$$

Where;

$h_c = \text{Target's Charateristic Dimension}$ [3]

2.3 Thermal Range Model (TRM)

The Thermal Range Model (TRM) which was developed and released by the Fraunhofer IOSB of Germany, which released version 4 v.2 in June of 2016 and is commonly referred to as TRM4. TRM4 expanded on the previous version, 3, or TRM3, by adding reflected and combined reflected and emitted radiation categories to the model [14]. Like with Johnson TRM4 is based on observation of 4 bar test target patterns and the range performance calculation is based on a modified version of Johnson's [14]. Unlike all the other metrics and models that have been or will be discussed herein TRM4 introduces two new terms. The first is the Average Modulation at Optimum Phase (AMOP) and the second is the Minimum Difference Signal Perceived (MDSP) [14, 15].

AMOP is used in place of the standard system MTF that has been previously discussed, due to MTFs inability to capture system aliasing artifacts and that MTF is the systems response to sine waves, not square waves or bar targets which for spatial sampling system such as starting Focal Plane Arrays causes sampling artifacts not captured by a standard MTF [14, 15]. There is "no analytical function for AMOP", but steps that can be used for each spatial frequency to determine AMOP and Table 4 lists these steps [14].

Table 4: AMOP Steps

(From [14])

Step	Task
1	Build a four-bar pattern signal and Fourier transform it
2	Multiply the Fourier transformed signal by the pre-filter MTF, i.e. the overall MTF of all components acting before the sampling process (turbulence, vibrations, optics, and detector)
3	Back transform the filtered signal to the spatial domain
4	Simulate the sampling of the pre-filtered four-bar pattern at different phases
5	Perform digital signal processing, zoom, and reconstruction on the signal
6	Fourier transform the reconstructed signal and multiply it by the post-reconstruction MTF (video processing, display, and eye MTFs)
7	Back transform the signal to represent the spatial output signal (at the brain level)
8	Determine the average modulation and the number of resolved bars at each phase
9	Find the optimum phase

The next part of TRM4 is the MDSP, which is the minimum signal (e.g. temperature for infrared systems) that an observer can perceive all bars in the target (standards are 3 or 4 depending on spectral band) at the optimum phase determined during AMOP. MDSP is defined by Equation 22.

$$\mathrm{MDSP} = \frac{\pi/2 * \mathrm{SNR_{th}} * \sqrt{\Psi_z(\mathrm{R,r})}}{\mathrm{AMOP_z(R,r)}} * \frac{3}{\mathrm{N_{pb}} - 1} \qquad \text{Equation 22 [14]}$$

Where;

$SNR_{th} = Threshold\ SNR\ of\ the\ eye$ [14]

$\Psi_z = Variance\ of\ the\ total\ noise\ perceived\ by\ the\ observer$

Note: TRM utilizes the Kornfeld-Lawson eye model over the more standard Barten eye model [3]

$z = Orientation\ of\ the\ pattern$

$r = Spatial\ frequency\ of\ pattern$

$R = Distance\ between\ imager\ and\ target$

$N_{pb} = Number\ of\ bars\ perceived$

While MDSP is a calculated number, at this point it should be pointed out that for well sampled imagers it is close to the MRTs or MRCs previously discussed [14]. Therefore MDSP can be measured in the lab, which like Johnson is extremely helpful for the purposes of relating real-world targets and ranges to laboratory measurable values.

In order to turn these values in to range performance data TRM4 uses Equation 23 and then used in the modified version of Equation 22 shown in Equation 24. This is related to a new metric that TRM4 defines as the Minimum Necessary Difference Signal (MNDS) as described in Equation 25. The last part of TRM4 is the Effective Difference Signal (EDS), shown in Equation 26, which is the difference in signal between the target and the background given atmospheric extinction as a function of wavelength and range [14]. Using these values TRM4 states that for the specified task as long and EDS is greater than MNDS the task is accomplished [14].

$$\mathrm{r_{p_z}} = \frac{\mathrm{n_{lp}}}{\mathrm{a_{tar_z}}} * \mathrm{R} \qquad \text{Equation 23 [14]}$$

Where;

$n_{lp} = Line\ paris\ needed\ per\ Johnson$

$a_{tar_z} = Target\ size\ (in\ z\ direction)$

$R = Range$

$$\mathrm{MDSP}\left(R, r_{p_z}\right) = \frac{\pi/_{2} * \mathrm{SNR_{th}} * \sqrt{\Psi_z(\mathrm{R}, r_{p_z})}}{\mathrm{AMOP_z}(\mathrm{R}, r_{p_z})} * \frac{3}{\mathrm{N_{pb}} - 1} \qquad \text{Equation 24 [14]}$$

$$\mathrm{MNDS_z}(\mathrm{R}) = \mathrm{MSDP}\left(\mathrm{R}, \mathrm{r_{p_z}}\right) \qquad \text{Equation 25 [14]}$$

$$\mathrm{EDS(R)} = \int \mathrm{DS}(\lambda, 0) * \tau_{\mathrm{atm}}(\lambda, \mathrm{R})\mathrm{d}\lambda \qquad \text{Equation 26 [14]}$$

TRM4 had two additional differences from United States developed legacy models. It corrected for target aspect, and used 1/f noise. This made some difference between the TRM3 and TRM4 versions and NVTherm 2002, but these have been corrected in the latest version of the model, NV-IPM [3]. A detailed comparison of NV-IPM, TRM4 as implemented in NV-IPM, and NVTherm 2002 [15]. Unfortunately the TRM4 components within NV-IPM have not been officially published due to only this single point of validation ([15]), so the planned comparison cannot be completed for TRM4, but relevant data can be observed in [15].

2.4 Target Task Performance Metric (TTPM)

In the decades since Johnson performed his research and the subsequent updates to Johnson and modeling theory using Johnson Criteria as a performance metric imaging system technology has changes extensively. Systems that were previously Direct View Optics (DVO) were replaced with digital imaging systems. In addition, digital imaging has gone through several generations of development resulting in most imaging applications today using digital imaging Focal Plane Arrays (FPAs), or a 2 dimension staring array of imaging pixels. The manufacturing technology of FPAs has also improved making the cost per pixel extremely affordable and in the case of some technology easy to manufacture. The result today is High Definition and even Ultra High Definition FPAs can be found in most spectral imaging bands. The move to digital imaging has also brought the capability of processing imagery prior to human consumption as well as better resolution.

As previously discussed Johnson Criteria uses a limiting resolution assumption, meaning that there is always enough target signal or target to background contrast available, but the resolution is the limiting factor in an imaging system [16, 17]. However, now that digital systems have developed beyond Time Delay Integration (TDI) scanning systems, and low resolution FPA technology, this is the not the case anymore. In 2006 it was realized that limiting resolution would no longer work well for performance predictions due to the technology advancements and modern FPA system being limited

by contrast and noise, specifically spectrally weighted noise due to frequency boost caused by image processing [6, 16, 17, 18]. The research began to replace Johnson Criteria with a performance metric that would correct this issue, along with a few other things that Johnson did not factor in. The result was the TTPM.

As previously alluded to in the Johnson Criteria section, Johnson utilizes MTF and CTF for range performance predictions and cycle criteria generation. The TTPM also uses similar methodology show in Equations 27, 28, and 29. Equation 27 is the base TTP calculation, however the adjustments in Equations 28 and 29 show the simplification of the various system level MTFs and CTFs into one relation of total system CTF to apparent target contrast.

$$TTP = \int_{\xi_{Low}}^{\xi_{Cut}} \sqrt{\frac{C_{tgt} * MTF(\xi)}{CTF(\xi)}}\, d\xi \qquad \text{Equation 27 [16]}$$

$$\mathrm{CTF}_{\mathrm{sys}}^{2} = \frac{CTF^{2}(\xi)}{MTF^{2}(\xi)} * \left(1 + \frac{\alpha^{2} * \sigma^{2}}{L^{2}}\right) \qquad \text{Equation 28 [16]}$$

$$\mathrm{TTP} = \int_{\xi_{\mathrm{Low}}}^{\xi_{\mathrm{Cut}}} \sqrt{\frac{\mathrm{C_{tgt}}}{\mathrm{CTF_{sys}}(\xi)}}\, \mathrm{d}\xi \qquad \text{Equation 29 [16]}$$

Where;

$C_{tgt} = Apparent\ Target\ Contrast$

$L = Display\ Luminance$

$\alpha = A\ calibration\ factor\ relating\ noise\ to\ Luminance$

$\sigma = RMS\ display\ noise$

Equation 29 is the most widely published version of the TTPM or V calculation. There has been an update to this equation with the publishing of the 2013 update to the TTPM. Equation 30 details this update. Equation 30 shows the addition of the actual target angle that is governed by Equation 31. The Equation 30 version of V was likely not widely adopted as earlier versions of the TTPM models locked θ_{tgt} at 15° whereas,

on the primary updated in the 2013 TTPM for NV-IPM was to correct this to make predictions more accurate.

$$V = \theta_{tgt} * \int_{\xi_{Low}}^{\xi_{Cut}} \sqrt{\frac{C_{tgt}}{CTF_{sys}(\xi)}}\, d\xi \qquad \text{Equation 30 [17, 19]}$$

$$\theta_{tgt} = \frac{\sqrt{a}}{R} \qquad \text{Equation 31 [17, 19]}$$

The last piece of information that is needed before Equation 30 can be applied the Target Transfer Probability Function (TTPF), the task difficulty characterization or V_{50} value, is required [17]. This V_{50} value is much like the N_{50} values that Johnson produced, and is often referenced as cycles in some literature. In order to generate V_{50} values for each task a forced choice experiment is used. This is similar to what Johnson did, except that for V_{50} observers undergo detailed training on what each task is defined as (Detection, Recognition, and/or Identification), and are required to pass a test on the training. The images shown are just of the target, i.e. there is no comparison to bar targets, and head location is controlled as to not induce changes in magnification to make better Detection, Recognition, or Identification calls [16, 20]. The targets in the selected target set are blurred at various levels to emulate range. Once the V_{50} values are obtained by forced choice experimentation, it is applied in the TTPF, Equation 32 and 33, which predicts the probability of task (Detection, Recognition, or Identification) performance.

$$P(Task) = \frac{\left({}^{V}/_{V_{50}}\right)^{E_{TTP}}}{1+\left({}^{V}/_{V_{50}}\right)^{E_{TTP}}} \qquad \text{Equation 32 [6]}$$

$$E_{TTP} = 1.51 + 0.24 * \left(\frac{V}{V_{50}}\right) \qquad \text{Equation 33 [6]}$$

Since all baseline values related to the TTPM are required to be captured by experimentation, it is expected that any change in model methodology will change some

of these values. In Equation 33, the 1.51 or A value, “determines the steepness of the psychometric function used to relate image quality to observer performance” and the 0.24 or B value, “determines the shape of the psychometric function used to relate image quality to observer performance” [19]. Since these values were related to the original TTP function, when the TTP function changes in 2013 and 2013 corrected an additional noise issue in the model the A and B values had to be updated for the 2013 version of the TTP to be A = 1.5 and B = 0 [17]. As maybe noticed Equations 32 and 33 are very similar to Equations 3 and 4 replacing N and N_{50} with V and V_{50}, and the A and B values in Equation 33.

One of the other major changes between Johnson and the TTPM methodology was that the TTPM used a bias in the probability model to correct for the observers ability to guess the task correctly [3]. In addition, Johnson Criteria had been used for a long time, and still had the benefit of relating system performance to lab measureable criteria, such as MRTs or MRCs. Therefore was an effort to relate TTPM to Johnson. Equation 34 was derived as link between the uncorrected for chance N_{50} from Johnson, and the new corrected for change V_{50} values.

$$V_{50} = 2.7 * N_{50} \qquad \text{Equation 34 [3]}$$

While Equation 34 was completed, published, used, and in a sense validated, it has been found to not be very accurate. This has been due to several reasons. As task definition, and target sets changed away from the standard Johnson targets to meet the modeling communities’ needs V_{50} became less and less linked to Johnson. It was also found that relating range performance to MRTs or MRCs predictions in the NVTherm models became less and less accurate with new technology that these predictions are no longer included in the standard modeling outputs in NV-IPM with the new 2013 TTPM. So, while the modeling verses field testing became more and more accurate with the TTPM and its 2013 updates, the V_{50} values have become less and less linked to values that can be measured in the lab, requiring field testing over lab measurements of MRTs or MRCs to validate system performance.

There have been many V_{50} perception studies done in the years since the TTPM was accepted into modeling practice. A number of tables could be built to include many of these values, however since a comparison of the different metrics is the goal of this research only the V_{50}'s that will be used in the upcoming sections will be included. These will be the ones linked as close as possible to the Johnson Criteria targets to come as close to a fair comparison as possible. Table 5 shows the main legacy TTPM values, however the man target was removed from the vehicle V_{50} study so it is not a direct conversion as Equation 34 assumes. Table 6 shows the updated V_{50} for the 2013 assumptions. The main fixes in the 2013 included the target angel and the noise calculations, and while the values in Table 6 make the tasks look easier the main reason for the fix as to correct for over predictions in produced by the legacy model caused by the noise and fixed target angle, which resulted in different psychometric function causing the A and B value changes and thus changes to the calculation of V, V_{50} and the Observer model using in NV-IPM [17].

Table 5: Legacy Target Task Performance (V50s) For Vehicles

(From [3])

Task	V50
Detection	2.7
Recognition	14.5
Identification	18.8

Table 6: 2013 Target Task Performance (V50s) For Vehicles

(From [13])

Task	V50
Detection	2
Recognition	9
Identification	13

3 Performance Model

Over the years there have been several iterations of sensor performance models using the metrics that have been discussed herein. They include AQUIRE, AQUIRE-LC, FLIR92, NVTherm, NVThermIP, SSCAMIP, IICAMIP, IINVD, TRM, and now the most

recent NV-IPM. Since many of the assumptions to the model were hard coded into the previous iterations of models, such as NVThermIP, when methodologies had to be updated so did the entire model. This made maintaining and developing models costly and hard to do. In addition, in the 2006 iteration of the United States developed models there were four different models to account for various spectral bands and technology. This meant that the community had to learn, update, and maintain four models all using various assumptions. For NV-IPM a great effort was made to change from a temperature space (FLIR92 and NVTherm) to a radiometric representation of the system, scene, and human [17]. This allowed for all four disparate models to be rolled into one common Graphical User Interface (GUI) and allowed for common code to be used throughout the model.

Since the intent was to replace all legacy models with a new model and abandon support for the legacy models the questions surfaces about being able to use NV-IPM to produce legacy model results, due in large part to the cost and time required to generate, through perception experimentation, new validated V_{50} values. To that end NV-IPM has the capability to reproduce results in NIIRS, FLIR92, NVTherm, and all four of the 2006 model variants. As previously mentioned a component of TRM was developed for IPM, but has yet to be officially published due to limited validation.

Figure 8 shows the GUI for NV-IPM. As can be seen the model GUI is divided into five different sections. The first is the Component Tree, an enlarged version can be seen in Figure 9, which shows all the components that are included in the model that is currently loaded. The first section is the target and background configuration which creates the target to background contrast that will be modeled; if this were a reflective band imager the illumination levels (Direct Sunlight, Full Moon, Clear Starlight, etc.) would be included. The next section covers the atmospherics, the first in this case Broadband Beer's law deals with the extinction of the signal to atmosphere and the second component, Turbulence MTF deals with the degradation of the image MTF due to atmospheric turbulence or C_n^2. The next section of the Component Tree has the imaging system and all the sub components that make up an imaging system, in this case a digital thermal imager. The last part is the observer and task performance

metrics. There are currently four loaded into the system, the three at the bottom of the Component Tree to represent Johnson, Legacy TTPM, and 2013 TTPM. The fourth is in the imaging system. Since NIIRS is defined by image interpretability by a human and does not include in the calculations as human components, it is place just after the imager or FPA of the system.

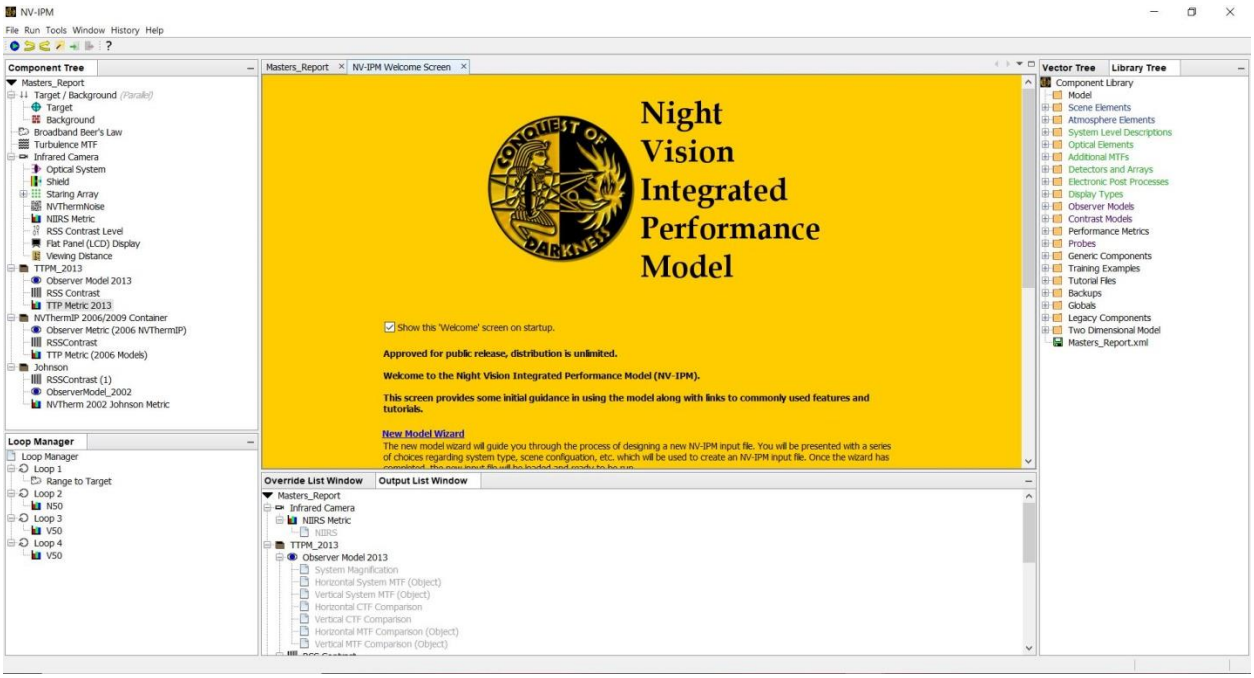

Figure 8: NV-IPM GUI

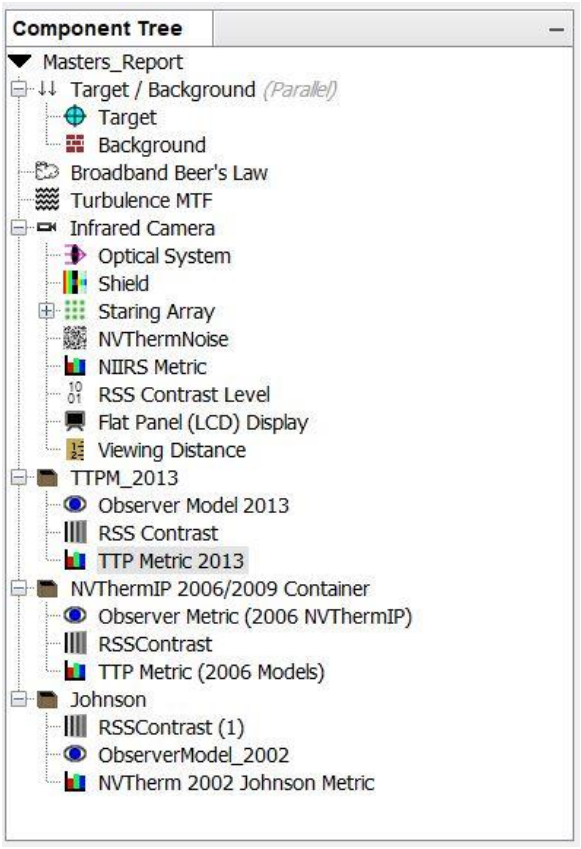

Figure 9: NV-IPM Component Tree

The lower left window in Figure 8 is the Loop Manager. NV-IPM allows the modeler to loop the model over full components, or individual entries, reducing the number of individual files, or runs have to be created. This is a very good improvement over the legacy models that only allowed one set of parameters to be run at a time. The far right window in Figure 8 has two tabs one call Library Tree, and the other Vector Tree. These are where the various pre-built components (noise, probes, MTFs, and all system characteristics) or vectors (irradiance, reflectivities, etc.) can be found and loaded into the Component Tree and then set as the system or model requires.

The bottom window in Figure 8 also has two tabs, one for a listing of all outputs the run is going to produce, and one for a list of all model overrides that are in the currently loaded model. Most calculated parameters in NV-IPM can be overridden, which is helpful when trying to compare the results of a system built in the model and measurements that are collected in the lab. For example one of the main overrides that

is commonly used in the modeling community is the system measured MTF. This allows for the comparison or as designed versus as built.

The last part of the GUI is the main window in the middle with the NVESD splash screen. As the modeler wishes to edit values of items of components, this is where the component edit windows will open.

4 Comparison

4.1 Modeled Imagers

Since there are variations in the definitions of NIIRS and differences in how noise is handled for legacy modeled observers between the infrared and visible, three sensors models were created for each spectral band. The each of the three sensor models are of varying resolution named; Lower Resolution, Mid Resolution, and Higher Resolution. Since most of the calculations in NV-IPM does not use format, but rely on detector pitch, that is the main value that changes between resolution settings. Modeling inputs for NV-IPM can be quite detailed, more detailed than is readily available via open source information. Therefore each detector was developed from numerous open source information and do not represent a single part number from a given manufacture, but represent the technology.

To avoid potential security issues the specific details of each imager's settings will not be included, but were derived from open source, foreign made sensor technology for the infrared and Commercial Off The Shelf (COTS) technology for the visible sensors. The developed sensors were then placed in front of the same lens system, keeping the effective focal length, aperture diameter, and transmission the same. While this is not necessarily accurate for visible versus infrared optical system, it will allow any comparisons among spectral bands. The visible sensor included a visible (400nm to 700nm) spectral cut filter, as well as Quantum Efficiency (QE) for each color channel to allow for the inclusion of demosaicing MTF blur.

4.2 Model Setup

The setup of the model as ran for the results on this paper is shown in Figure 10.

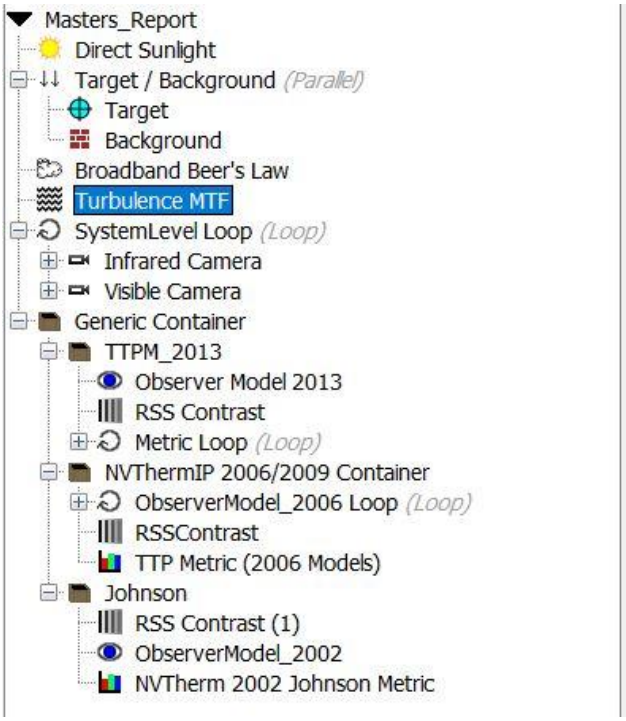

Figure 10: NV-IPM As Built Component Tree

In order to accommodate the running of a visible imager an illumination condition had to be selected. At first pass, since the goal is compare the results of various performance metrics and not stress the imager itself, a high illumination condition, Direct Sunlight, was selected. This selection was from the standard available spectral illuminations conditions found in the Vector Library of NV-IPM.

The next part of the model is the target and background. This defines the Characteristic Dimension discussed previously and the thermal and reflective contrasts. The values for the dimension and thermal contrast were assigned per reference 13 and a flat reflectivity values for the target and background were selected. The atmosphere was set using Beer's Law for a high transmission value, and the C_n^2 was set to a Very Low value due to the goal being metric comparison not performance of the sensors.

The last part was the setup of the various metrics. For times when legacy metrics are needed in NV-IPM the various metric and observer models have been developed and included to emulate the legacy models. For that reason, Figure 10 shows a Generic Container with the loops, metrics and observers for each of the desired metrics. This includes the 2002 Johnson, Legacy TTPM, and the 2013 TTPM. One item to note is that the legacy TTPM container has a loop in the observer model. This is due to NVThermIP and SSCAMIP having different noise settings for the observer, an issue that was discussed above, and will be shown in the next section.

Figure 11 shows the metric loops that were setup and the N_{50} and V_{50} values used for this comparison. As discussed in previous sections these are the closest representation of the target of interest for a fair comparison of metric results.

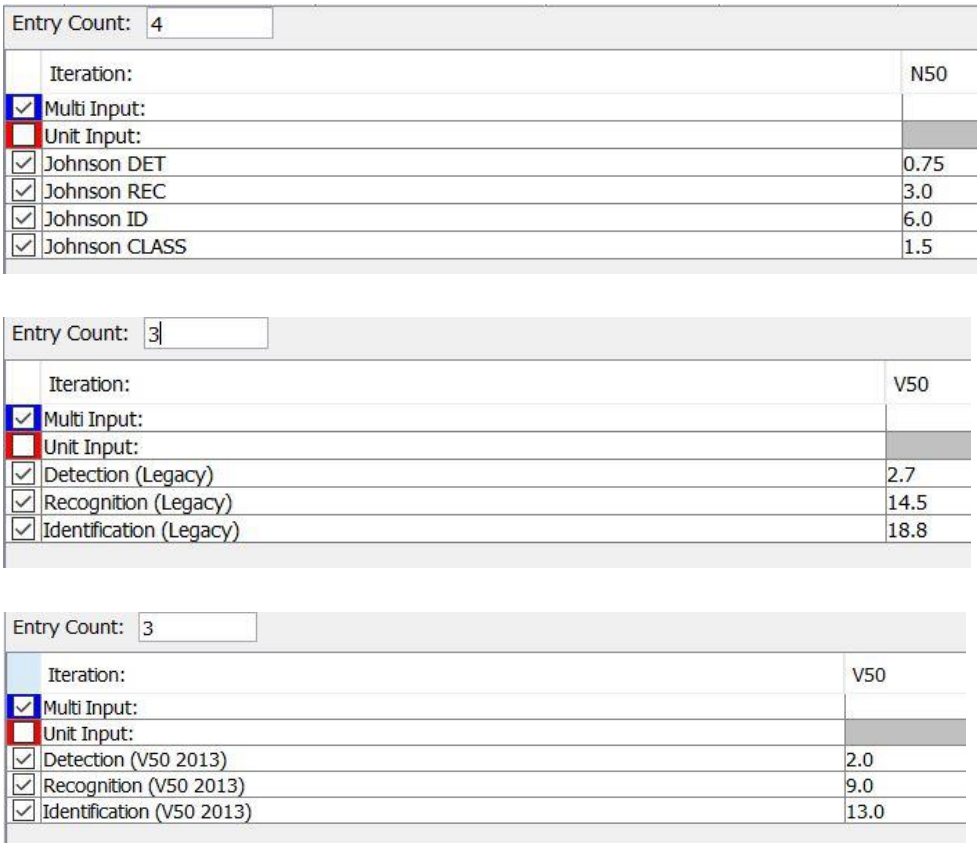

Figure 11: NV-IPM Metrics Loop Settings

(a) Johnson Criteria Loop Settings, (b) Legacy TTPM Loop Settings, (c) 2012 TTPM Loop Settings

4.3 Results

The last note that needs to be provided prior to showing or discussing the results included herein is about range. Due to potential concerns related to security for actual performance of sensors, the range has been scaled from that returned from NV-IPM to a neutral set of values between 0 and 1. The MATLAB script that generated the plots herein has not been provided to mask the scaling so the actual range results cannot be recovered.

The first item that needs to be discussed is the reference in several references and equations, specifically to Equations 7, 8, and 21 that reference a comparison of resolution to Johnson Criteria. The first comparison that that needs to be done before diving too deep into the metrics is this comparison of N as it relates to resolution. In that context, Equation 21 was applied using the targets characteristic dimension and the GSD outputs from NV-IPM in the NIIRS metric list of available outputs. Figures 12 and 13 plot Equation 21's definition of N as a function of resolution to that of N calculated by NV-IPM's NVTherm 2002 Johnson Metric that uses the CTF methodology previously shown in Figure 7. As can be seen in Figures 12 and 13, the CTF methodology provides a much greater N value, especially at shorter range.

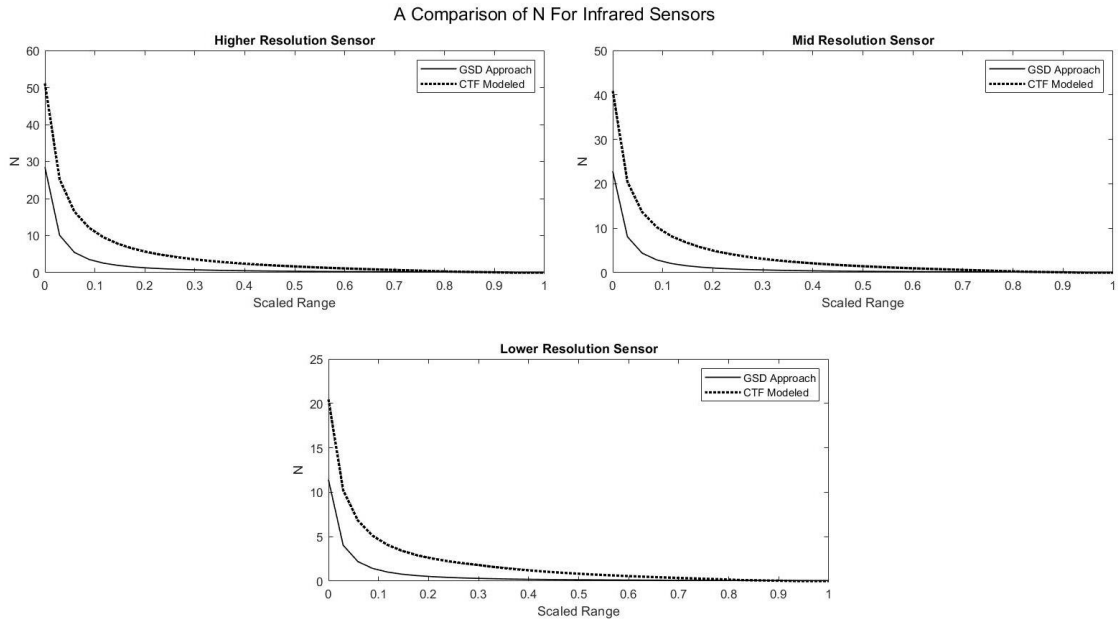

Figure 12: N Comparison For Infrared Sensors

(a) Higher Resolution, (b) Mid Resolution, (c) Lower Resolution

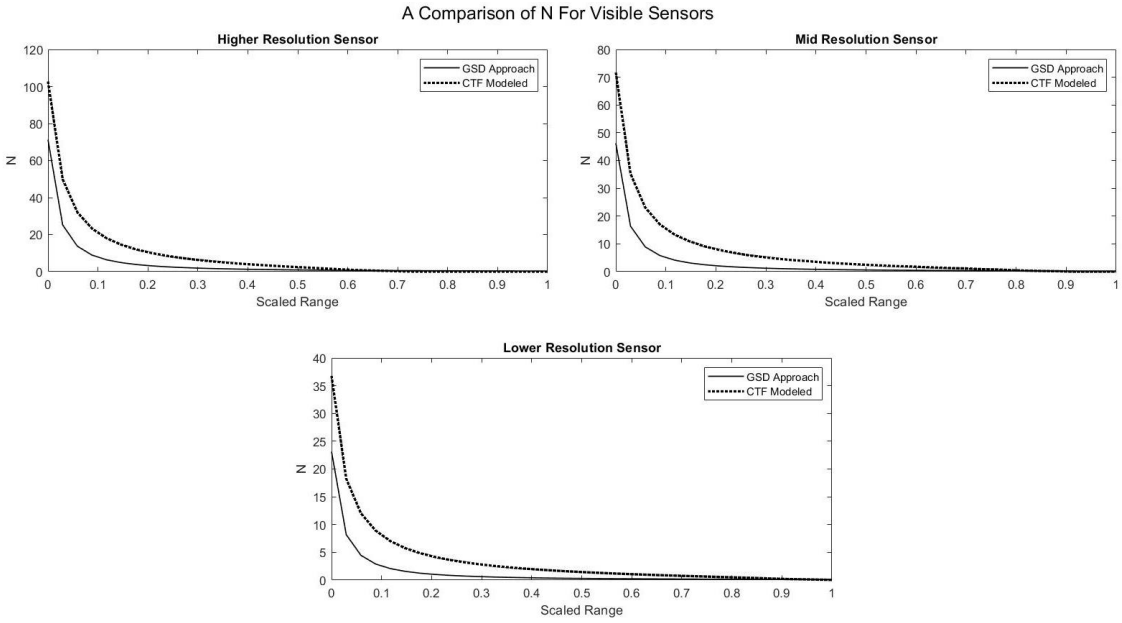

Figure 13: N Comparison For Visible Sensors

(a) Higher Resolution, (b) Mid Resolution, (c) Lower Resolution

Going back to Equation 3 and 4 which describes the calculations for P(Task) and E_j it is known that the performance is tied, in the numerator of the equations to N at each range. Thus the pixels on target approximation going to under predict standard Johnson Criteria in this case. This is due to the pixels on target not accounting for any contrast in the target the way Johnson was applied with the application of MRTs/MRCs or CTF in the modeling applications. In addition since the pixels on target calculations rely on the GSD of the system, which in NV-IPM is calculated in the NIIRS Metric part of the model none of the contrast, MTF, or magnification calculations due to the items that come after the FPA in the imaging system are taken into account, such as the display and RSS Contrast (image processing). When the N values from the GSD approach are applied to Equations 3 and 4, Figures 14 through 19 show the comparison of the Pixels on Target P(Task) calculations against those P(Task) as determined by the Modeled Johnson Criteria. As can be seen in these Figures, and as expected through investigation into NIIRS the resolution to performance comparisons is not very accurate.

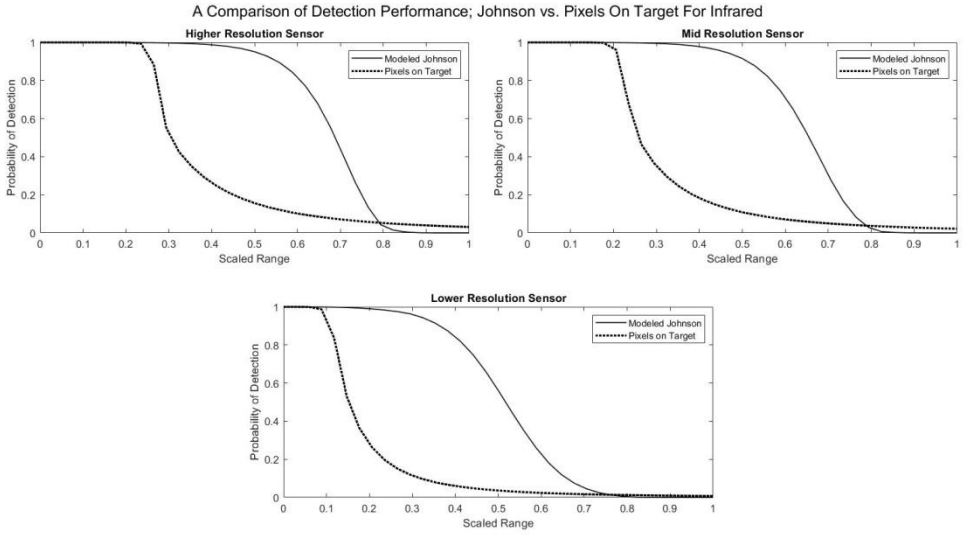

Figure 14: Johnson Detection and Pixels on Target Comparison For Infrared Sensors

(a) Higher Resolution, (b) Mid Resolution, (c) Lower Resolution

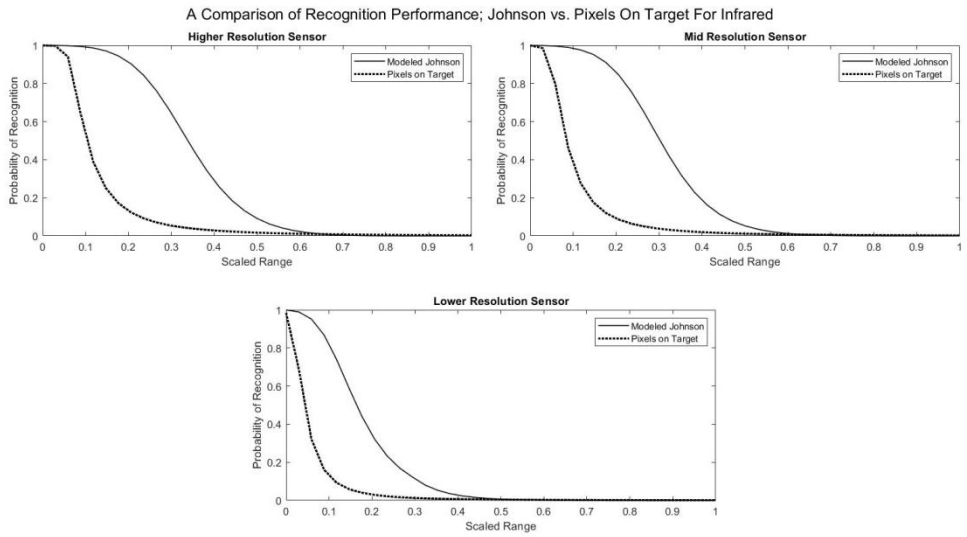

Figure 15: Johnson Recognition and Pixels on Target Comparison For Infrared Sensors

(a) Higher Resolution, (b) Mid Resolution, (c) Lower Resolution

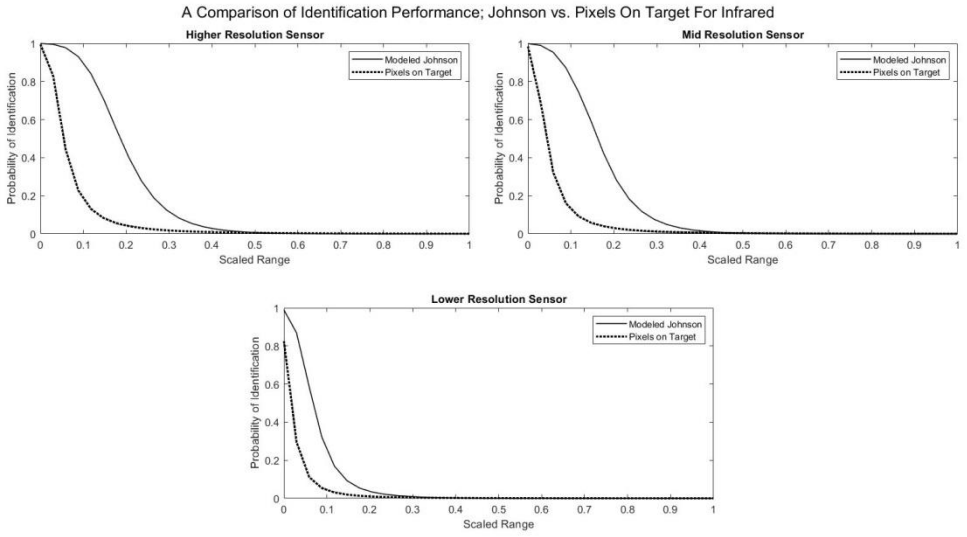

Figure 16: Johnson Identification and Pixels on Target Comparison For Infrared Sensors

(a) Higher Resolution, (b) Mid Resolution, (c) Lower Resolution

Figure 17(a) did return an interesting result. As can be observed there is a cross over from the two different approaches at a fairly higher level of P(Task), in this case Detection. The original intent of the 2002 NVTherm software was not for visible imagers. It is possible that the Observer Metric for 2002 also had similar issues to that of the

Legacy TTPM that are causing some interesting results for the Higher Resolution sensor. The older Observer Metric was used in the model to ensure results from Johnson were calculated in accordance with models built upon the Johnson premise.

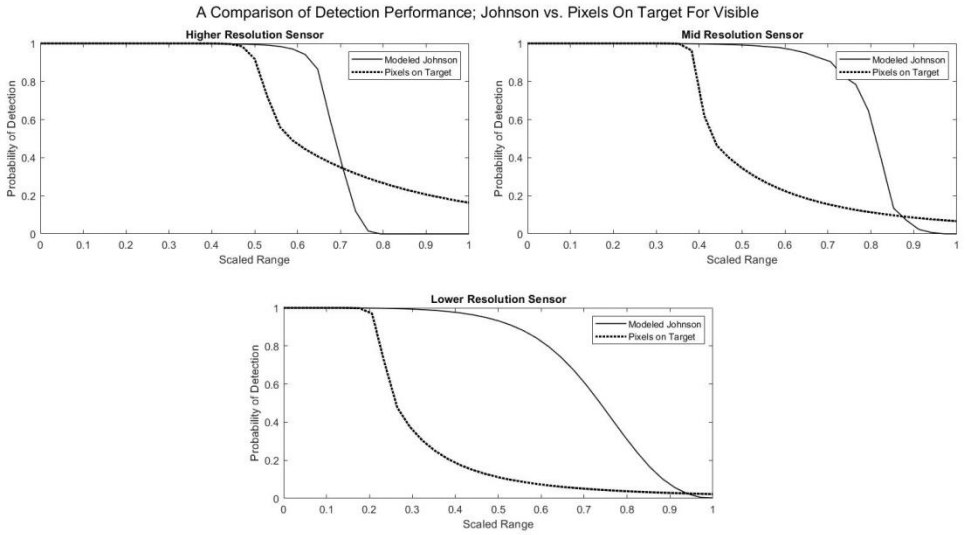

Figure 17: Johnson Detection and Pixels on Target Comparison For Visible Sensors

(a) Higher Resolution, (b) Mid Resolution, (c) Lower Resolution

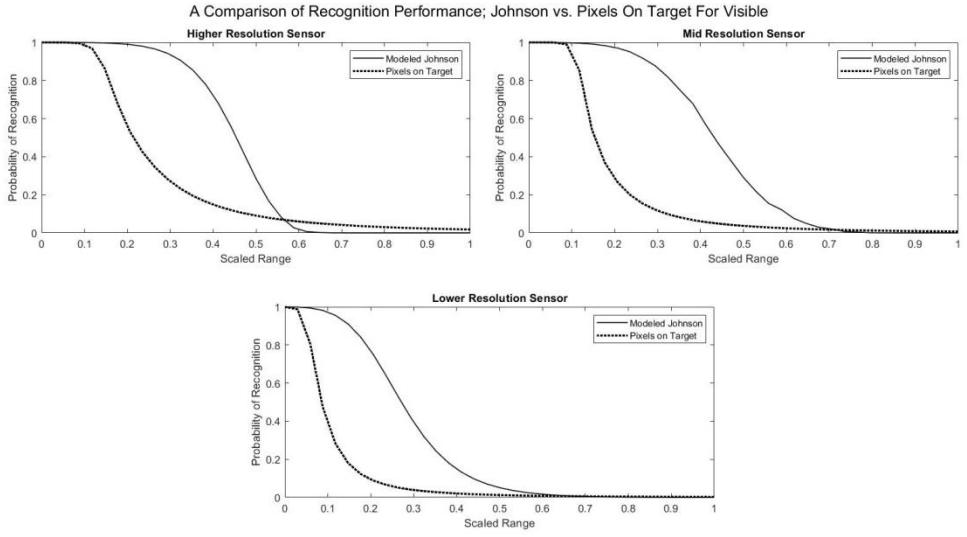

Figure 18: Johnson Recognition and Pixels on Target Comparison For Visible Sensors

(a) Higher Resolution, (b) Mid Resolution, (c) Lower Resolution

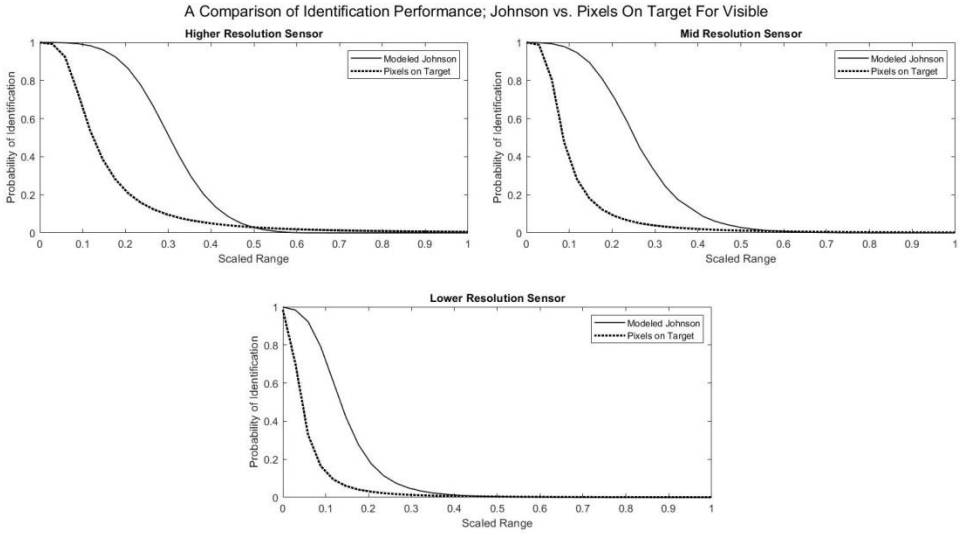

Figure 19: Johnson Identification and Pixels on Target Comparison For Visible Sensors

(a) Higher Resolution, (b) Mid Resolution, (c) Lower Resolution

Figures 20, 21, and 22 plot the three primary metrics for P(Task); Johnson, Legacy TTPM, and 2013 TTPM; for the infrared systems. Figure 20, Detection, for the various resolutions that Johnson tracks quite closely with the Legacy TTPM results until a point and then trails off from the Legacy TTPM, whereas the 2013 TTPM produces lower results from the other two metrics. This is due to the Johnson Observer Metric producing a CTF amplitude similar to that of the Legacy TTPM, but having a much steeper curve leading to the emulation of the 2013 TTPM Observer and P(Task) results at higher spatial frequencies specifically for Detection. For the other two metrics the Legacy TTPM and 2013 TTPM have decent correlation, which was expected [17]. However, the Johnson model seems to transition from a correlation with the Legacy TTPM to under predicting the 2013 TTPM.

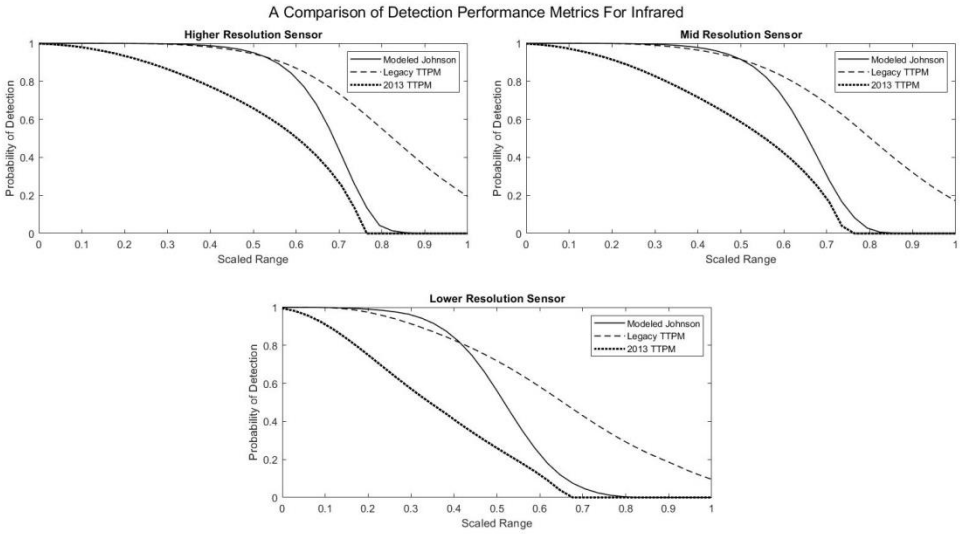

Figure 20: Detection Performance Comparison For Infrared Sensors

(a) Higher Resolution, (b) Mid Resolution, (c) Lower Resolution

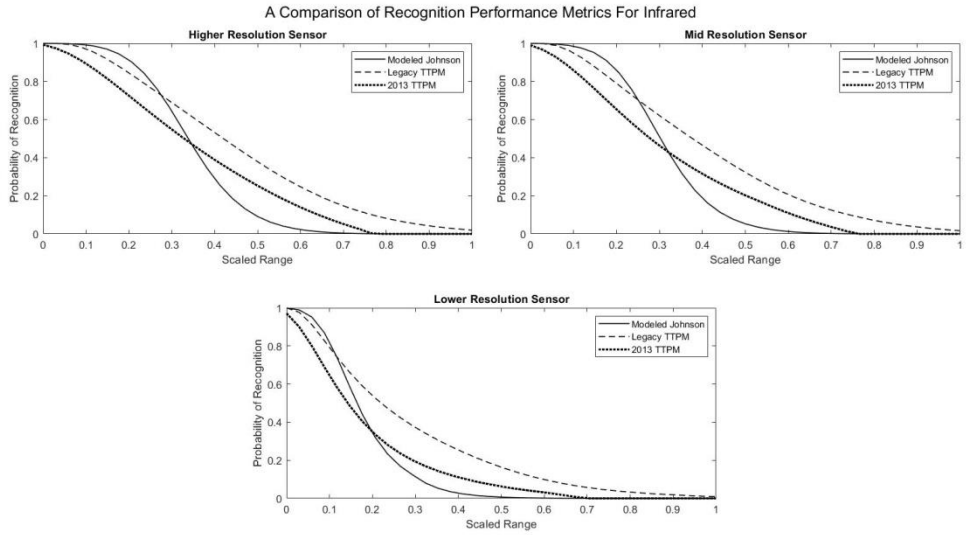

Figure 21: Recognition Performance Comparison For Infrared Sensors

(a) Higher Resolution, (b) Mid Resolution, (c) Lower Resolution

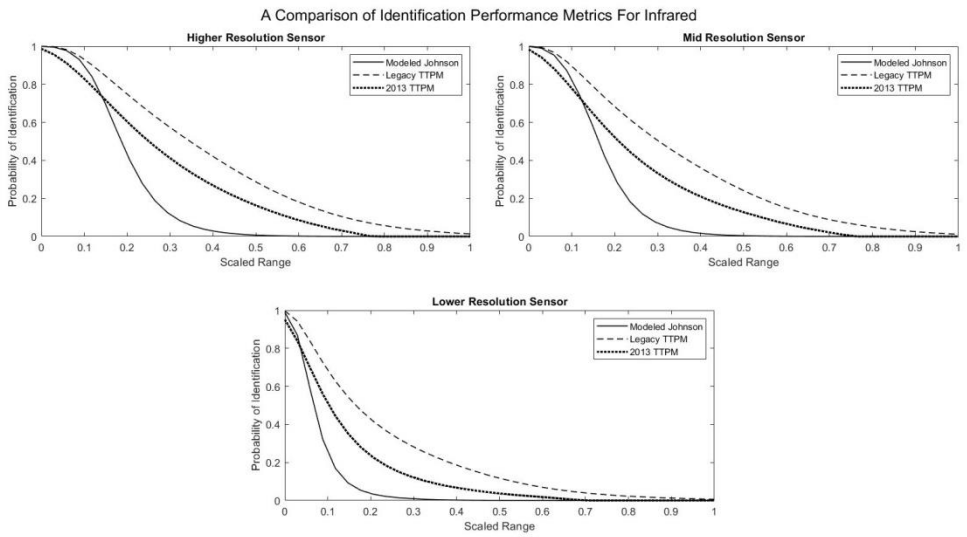

Figure 22: Identification Performance Comparison For Infrared Sensors

(a) Higher Resolution, (b) Mid Resolution, (c) Lower Resolution

Figures 23, 24, and 25 show the comparisons of the three P(Task) metric results for Detection, Recognition, and Identification of the target that was modeled for the visible imagers. As expected the visible Observer Model used in the Legacy TTPM models causes a large delta in the performance predictions for the Legacy TTPM as opposed to the other modeled metrics [17]. This is especially apparent in the Detection task as it far over preforms the Johnson Detection predictions. However, it is interesting to observe the results for the Recognition and Identification tasks. In the Recognition Task at lower probabilities Johnson seems to track along with the 2013 TTPM predictions, which for Identification it under predicts performance compared to the 2013 TTPM predictions.

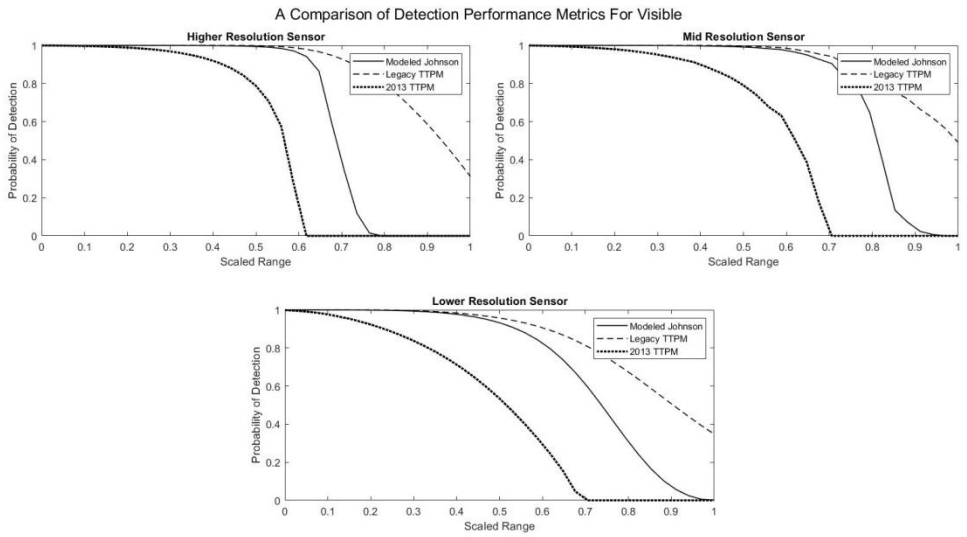

Figure 23: Detection Performance Comparison For Visible Sensors

(a) Higher Resolution, (b) Mid Resolution, (c) Lower Resolution

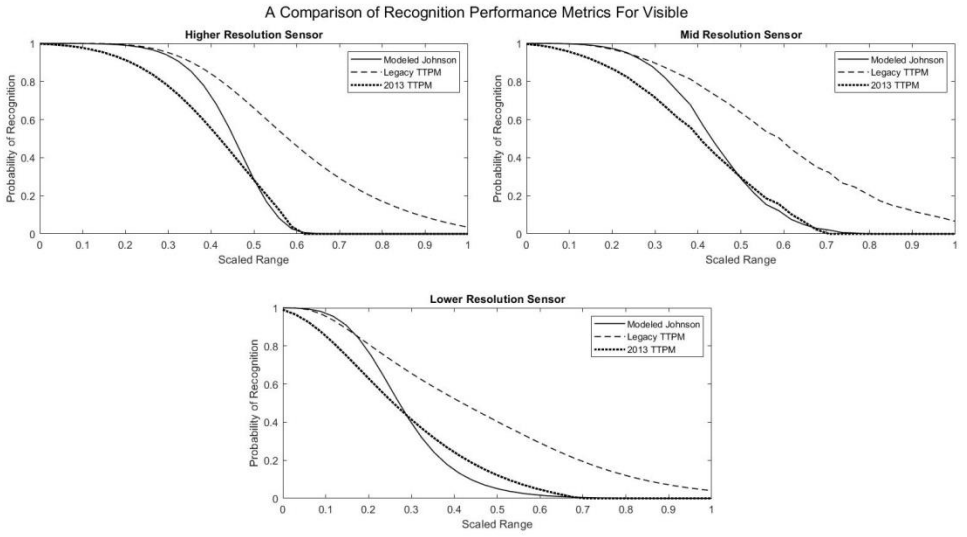

Figure 24: Recognition Performance Comparison For Visible Sensors

(a) Higher Resolution, (b) Mid Resolution, (c) Lower Resolution

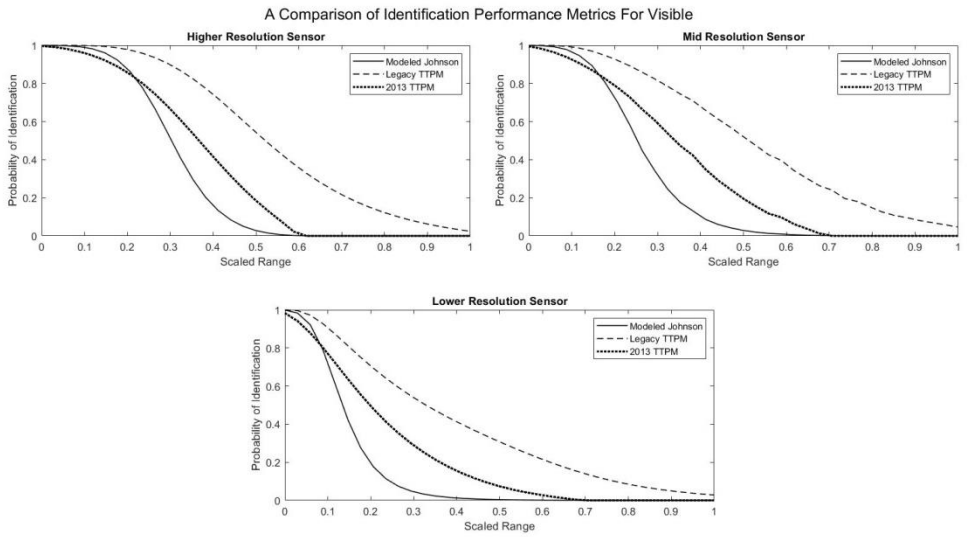

Figure 25: Identification Performance Comparison For Visible Sensors

(a) Higher Resolution, (b) Mid Resolution, (c) Lower Resolution

The next comparison this is going to be added herein is to add the comparison of the performance predictions to NIIRS. Figures 26 – 31 display the results from the previous figures, but now with NIIRS plotted along the secondary y-axis. NIIRS is a zero to nine absolute scale and so is probability from zero to one. So, it was reasoned that they could be plotted in a double y-axis plots for comparison. The other item that was added to the plots was the approximate NIIRS rating for each task; i.e. NIIRS of 5 for infrared Detection, NIIRS of 6 for infrared Recognition, NIIRS of 7 for infrared Identification, NIIRS of 3 for visible Detection, NIIRS of 4 for visible Recognition, and NIIRS of 6 for visible Identification. These were approximated based on Table 8, as the specific description related to the Johnson and TTPM definitions of these tasks are not exact matches to the NIIRS definitions. Since NIIRS is a single output from the NV-IPM software, and not dependent on task, the NIIRS curves are the same for all tasks. What is being observed is if or where the selected NIIRS rating, NIIRS prediction, and P(Task) converge. As can be seen in Figures 26 and 29 there is not good correlation for the Detection, task for either spectral band. Figures 27 and 30 also do not have good correlation, but the lower resolution sensors are showing better than the other sensors. Figure 28 and 31 again show little correlation.

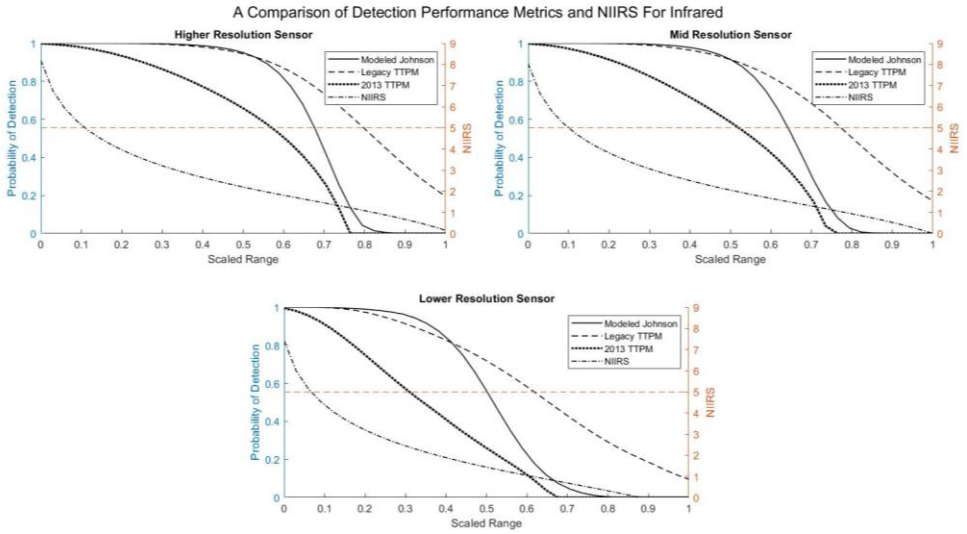

Figure 26: Detection Performance and NIIRS Comparison For Infrared Sensors

(a) Higher Resolution, (b) Mid Resolution, (c) Lower Resolution

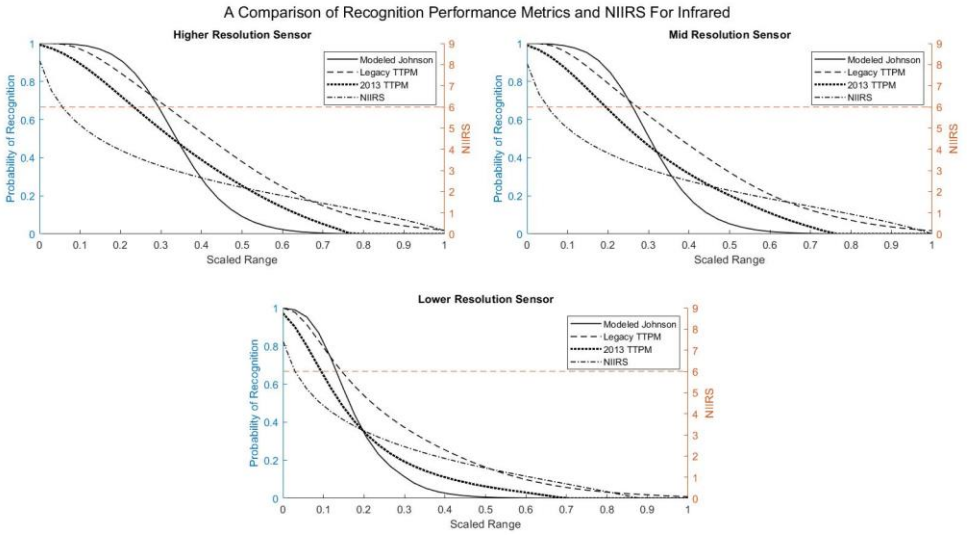

Figure 27: Recognition Performance and NIIRS Comparison For Infrared Sensors

(a) Higher Resolution, (b) Mid Resolution, (c) Lower Resolution

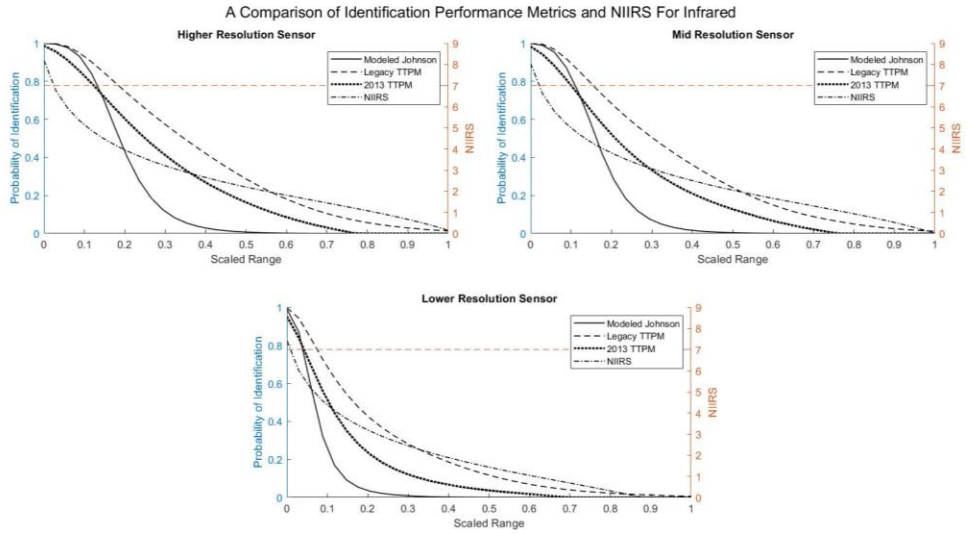

Figure 28: Identification Performance and NIIRS Comparison For Infrared Sensors

(a) Higher Resolution, (b) Mid Resolution, (c) Lower Resolution

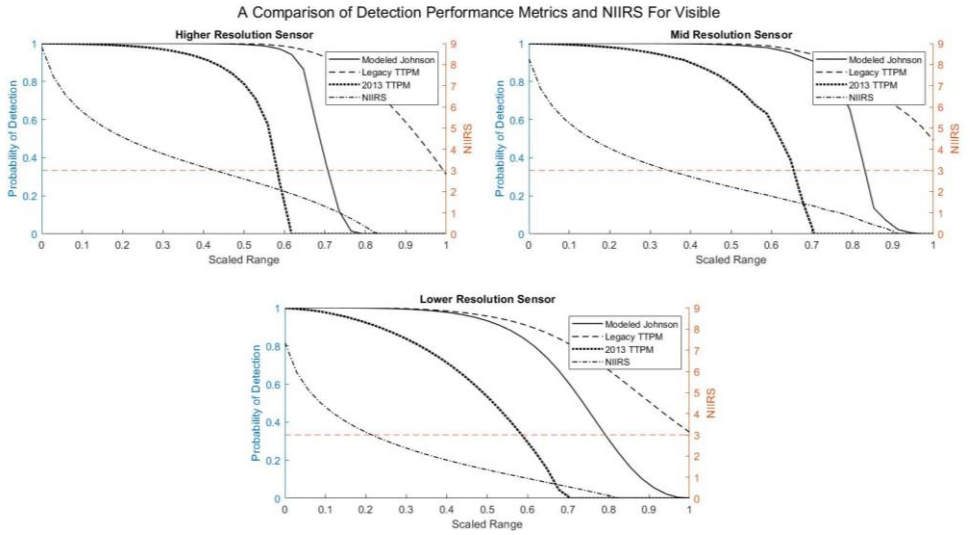

Figure 29: Detection Performance and NIIRS Comparison For Visible Sensors

(a) Higher Resolution, (b) Mid Resolution, (c) Lower Resolution

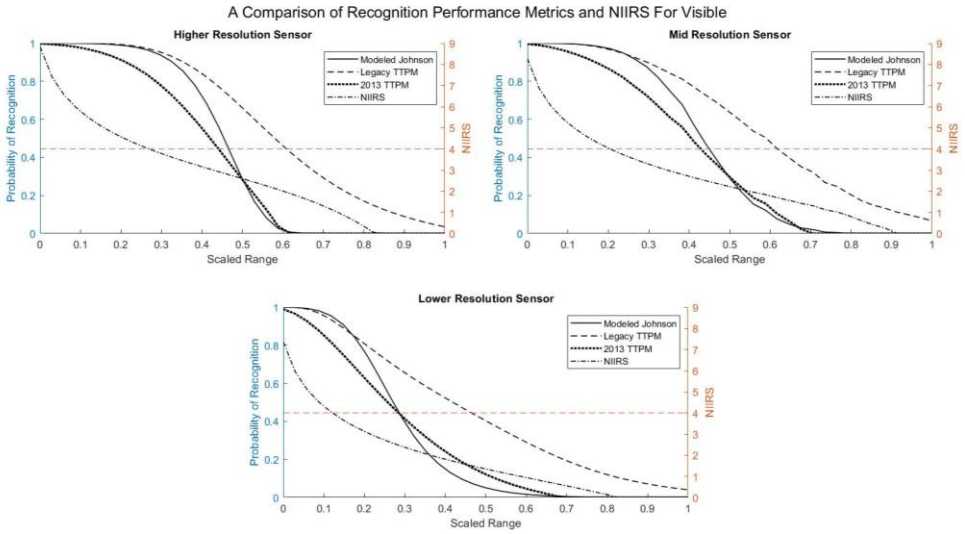

Figure 30: Recognition Performance and NIIRS Comparison For Visible Sensors

(a) Higher Resolution, (b) Mid Resolution, (c) Lower Resolution

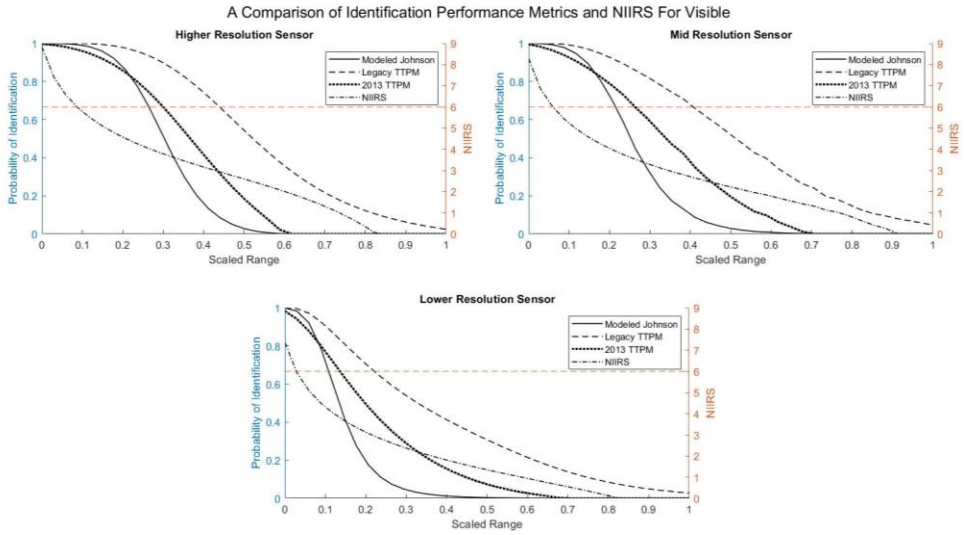

Figure 31: Identification Performance and NIIRS Comparison For Visible Sensors

(a) Higher Resolution, (b) Mid Resolution, (c) Lower Resolution

The last series of results that can be compared comes from the concepts that relate Pixels on Target assumptions to NIIRS [10]. For Figures 32 – 37 the N values that were previously calculated using the GSD methodology are plotted on a two y-axis scale with the NIIRS results. With this approach there is a much better correlation to the

predictions and the required NIIRS rating for each task, with the exception of Detection. This shows that the assumptions are correct that pixels on target and Johnson are a good fit with NIIRS assuming that SNR, contrast, image processing, and display parameters are ignored [10]. These plots also show that while for certain tasks a P(Task) at a required NIIRS does have correlation to the NIIRS predictions the rest of the plots do not correlate well. This leads back to the realization that resolution alone is not a good predictor of performance, hence the rationale to replace IIRS with NIIRS and the transition from Johnson to TTPM.

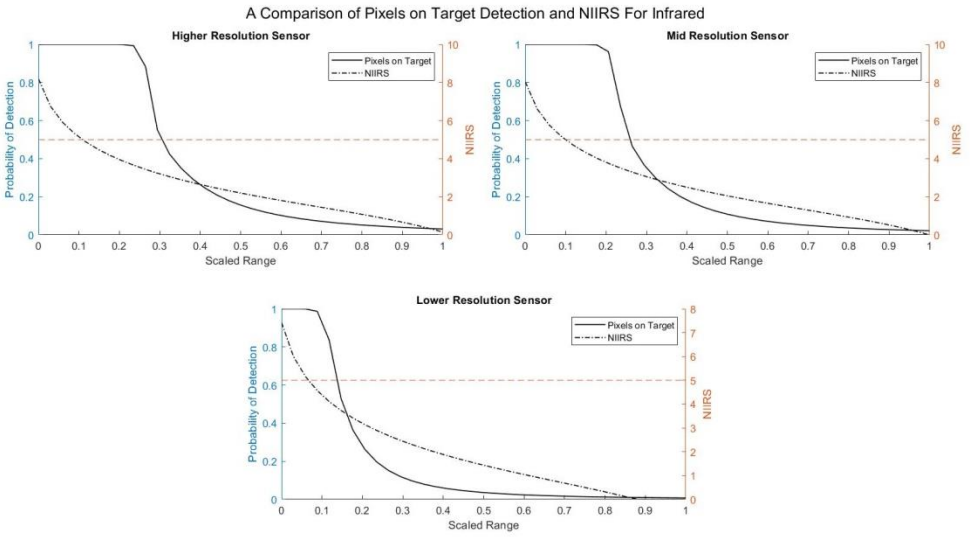

Figure 32: Pixels on Target Detection and NIIRS Comparison For Infrared Sensors

(a) Higher Resolution, (b) Mid Resolution, (c) Lower Resolution

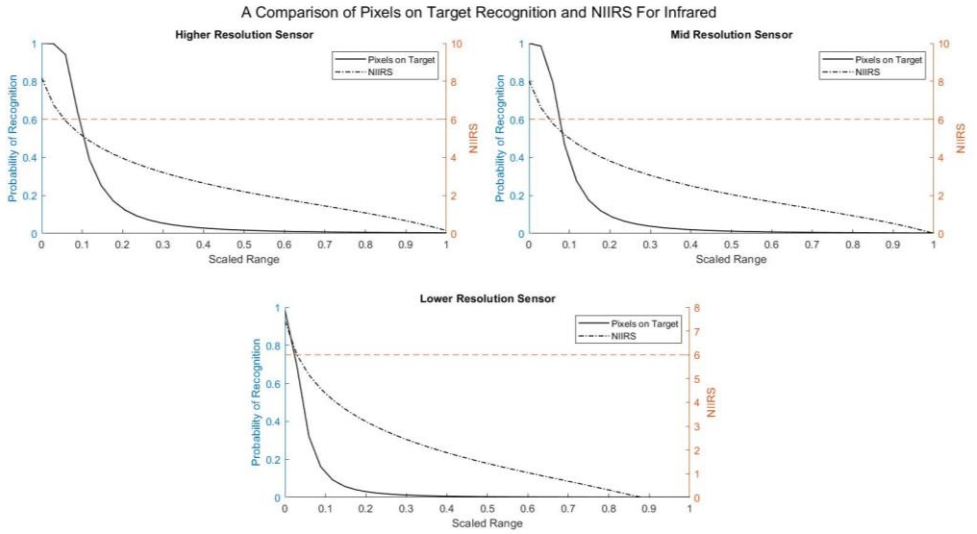

Figure 33: Pixels on Target Recognition and NIIRS Comparison For Infrared Sensors

(a) Higher Resolution, (b) Mid Resolution, (c) Lower Resolution

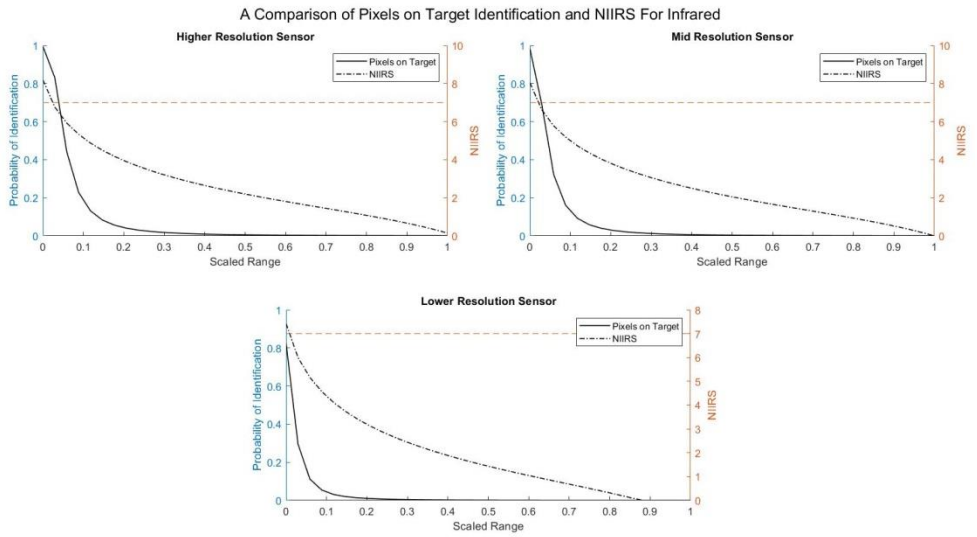

Figure 34: Pixels on Target Identification and NIIRS Comparison For Infrared Sensors

(a) Higher Resolution, (b) Mid Resolution, (c) Lower Resolution

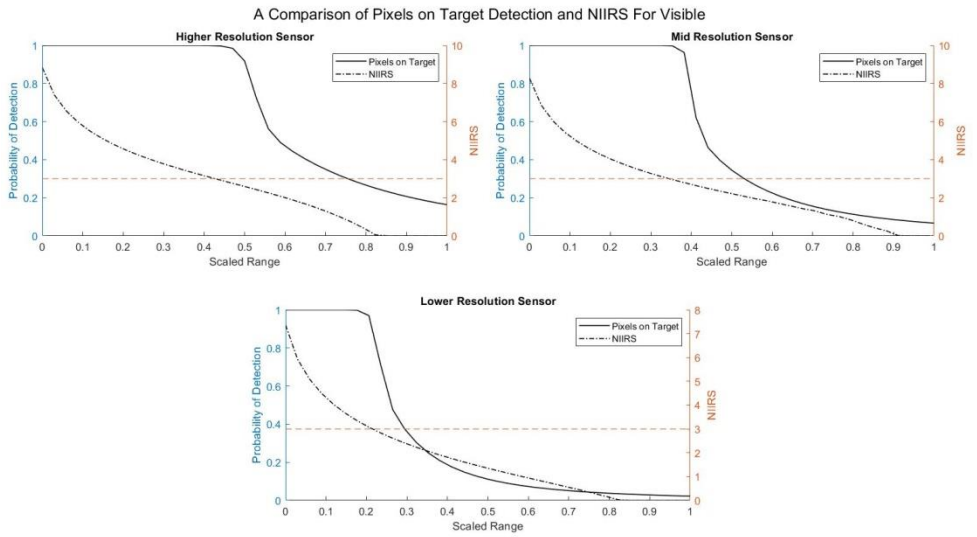

Figure 35: Pixels on Target Detection and NIIRS Comparison For Visible Sensors

(a) Higher Resolution, (b) Mid Resolution, (c) Lower Resolution

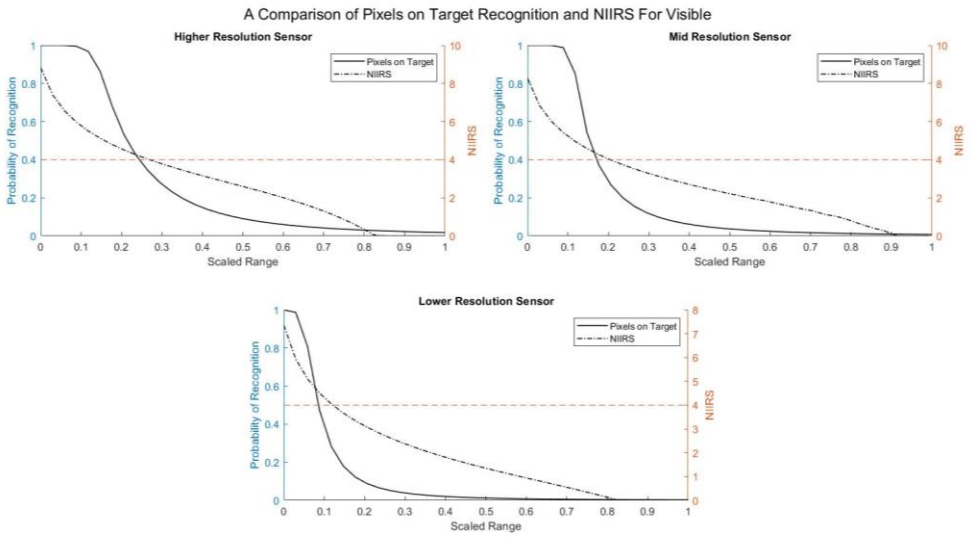

Figure 36: Pixels on Target Recognition and NIIRS Comparison For Visible Sensors

(a) Higher Resolution, (b) Mid Resolution, (c) Lower Resolution

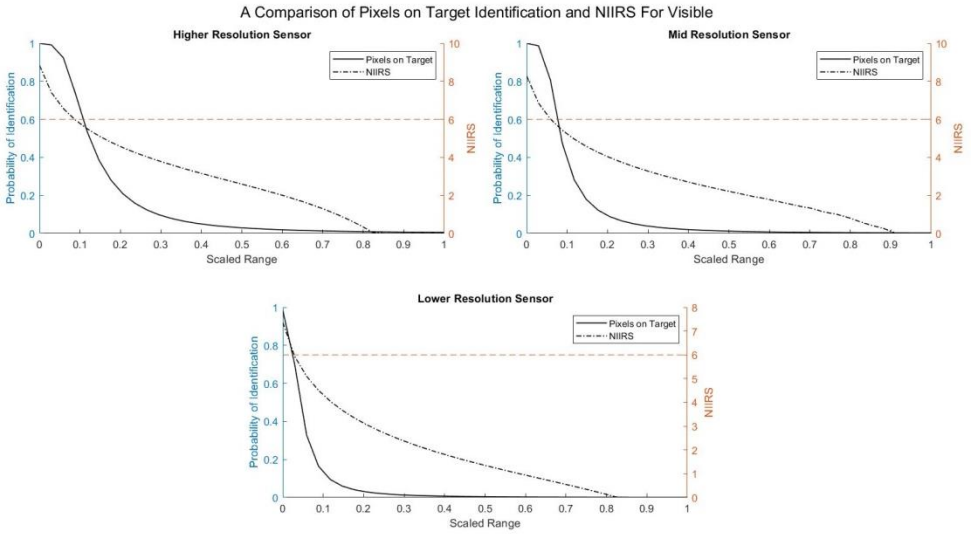

Figure 37: Pixels on Target Identification and NIIRS Comparison For Visible Sensors

(a) Higher Resolution, (b) Mid Resolution, (c) Lower Resolution

5 Conclusions

Modeling and simulation of imaging sensors as grown, change, and diverged over the years of development. The first item that conclusion that can be drawn is the metrics developed for different applications NIIRS versus P(Task) cannot fairly be compared. There is too much difference in the result dependences, the definition of tasks, and the lack of reliance on NIIRS predictions related to image processing the display or the observer. The mapping of NIIRS to P(Task) required that major contributing factors to actual system performance; contrast, SNR, CTF, magnification, etc. be ignored. This results in a better collection, but poor prediction of actual system performance.

The next item we can look at is relating resolution solely to P(Task). While it is documented, much like the comparison to NIIRS it relies on ignoring everything related to the target, except size, whereas the implementation of system modeling relies on CTF this will provide very poor performing systems, or if the designer relies on this “relationship” will lead to the design being far and above in complexity and cost than is actually required. Since CTF is tied to the contrast of the target the relationship may

need to be reevaluated with decreasing contrast between the target and background as the original input.

The last item is that changes in the Observer Metric over the years have caused some interesting results to be noticed in the plots. The first observation is that the Legacy TTPM and its observer metric should not be used for visible imaging applications. The Legacy TTPM showed a wide delta in performance from that of both Johnson and the 2013 TTPM. This was one of the main reasons for the change. The infrared systems had a better correlation between the Legacy TTPM and the 2013 TTPM for Recognition and Identification. The Johnson results seem to under predict Identification compared to the Legacy TTPM and 2013 TTPM, land between the two for Detection, and have a mixed correlation for Recognition. These results lead to the conclusion that as previously discussed Johnson is not a good metric especially for the higher resolution sensors and the Legacy TTPM has numerous problems, so the 2013 TTPM seems to be the best all-around metric and Observer model for modeling P(Task).

With that said P(Task) modeling was still originated for lower altitude modeling, NIIRS still has a place for sensor performance for specific applications. The key take away from this is that the signal and contrast impact system performance greatly. The simplification of imager performance to resolution simply does not work. Designing systems based on this relationship does not account for the full implementation of the system. Contrast and magnification (or other display parameters) play an important role in system performance and cannot simply be ignored.

As a final statement the metrics that should be utilized in performance modeling of human in the loops optical systems should be the 2013 TTPM and NIIRS depending on the application and information available. Yes, the TTPM metric relies on experimental derivation of its V_{50} value and is not directly lab measureable, however it has developed over the years to correct the issues found in Johnson and the Legacy TTPM and with validated V_{50} values will give the most accurate predictions of imager performance with compared to range observations. In addition with all of the variation in

Detection results, it may be necessary to direct research into how Detection is assessed in the realm of modeling and simulation of imager performance. There is a lot of variation in results and it is possible Johnson, nor TTPM may be the best answer to modeling Detection performance.

6 References

[1] Burgener, M. (2020). *Broadband Infrared Objective Lens Homework #6.* University of Arizona.

[2] Baum, I. (2013, November 8). *File:USAF-1951.svg.* Retrieved March 13, 2021, from Wikimedia Commons: https://commons.wikimedia.org/wiki/File:USAF-1951.svg

[3] Host, G. C. (2008). *Electro-Optical Imaging System Performance (Fifth Edition ed.)*. Bellingham, Washington, USA: SPIE and JCD Publishing.

[4] Holst, G. C. (2003). *Holst's Practical Guide to Electro-Optical Systems*. Winter Park, FL, USA: JCD Publishing.

[5] Leachtenauer, J. C. (2003). *Resolution Requirements and the Johnson Criteria Revisited*. In G. C. Holst (Ed.), SPIE AeroSense 2003; Infrared Imaging Systems: Design, Analysis, Modeling, and Testing XIV. Proceedings of SPIE Vol. 5076. Orlando: SPIE.

[6] Daniels, A. (2018). *Field Guide to Infrared Systems, Detectors, and FPAs (Third Edition ed.)*. Bellingham, Washington, USA: SPIE.

[7] Night Vision Electronic Sensors Directorate (NVESD). (n.d.). *Night Vision - Integrated Performance Model (NV-IPM) Johnson Metric 2020 Help*. Night Vision - Integrated Performance Model (NV-IPM), 1.11. NVESD.

[8] Irvine, J. M. (1997). *National Imagery Interpretability Rating Scales (NIIRS): Overview and Methodology*. SPIE Optical Science, Engineering and Instrumentation; Airborne Reconnaissance XXI. Vol. 3128. San Diego: SPIE.

[9] Bai, H. (2011). *Research on Quantitative Relationship Between NIIRS and the Probabilities of Discrimination*. In J. J. Puschell, J. Chu, & J. Lu (Ed.). Proc. of SPIE Vol. 8193. SPIE International Symposium on Photoelectronic Detection and Imaging; Advances in Infrared Imaging and Applications: SPIE.

[10] Driggers, R. G., Kelley, M., & Cox, P. G. (1996). *National Imagery Interpretation Rating System (NIIRS) and the Probabilities of Detection, Recognition, and Identification.* SPIE Aerospace/Defense Sensing and Controls; Infrared Imaging Systems: Design, Analysis, Modeling, and Testing VII. Vol. 2743 1349. Orlando: SPIE.

[11] Young, D., Yen, J., Bakir, T., Brennan, M., & Butto Jr., R. (2009). *Video National Imagery Interpretability Rating Scale Criteria Survey Results*. In D. J. Henry (Ed.), SPIE SPIE Defense, Security, and Sensing; Airborne Intelligence, Surveillance

Reconnaissance (ISR) Systems and Applications VI. Proc. of SPIE Vol. 7307. Orlando: SPIE.

[12] Night Vision Electronic Sensors Directorate (NVESD). (n.d.). *Night Vision - Integrated Performance Model (NV-IPM) NIIRS Metric Help*. Night Vision - Integrated Performance Model (NV-IPM), 1.11. NVESD.

[13] Night Vision Electronic Sensors Directorate (NVESD). (n.d.). *Night Vision - Integrated Performance Model (NV-IPM) NV-IPM Recommended V50 Table*. Night Vision - Integrated Performance Model (NV-IPM), 1.11. NVESD.

[14] Keβler, S., Gal, R., & Wittenstein, W. (2017). *TRM4: Range Performance Model for Electro-Optical Imaging Systems*. In G. C. Holst, & K. A. Krapels (Ed.), SPIE Defense + Security; Infrared Imaging Systems: Design, Analysis, Modeling, and Testing XXVIII. Proc. of SPIE Vol. 10178. Anaheim: SPIE.

[15] Teaney, B. P., Reynold, J. P., Du Bosq, T. W., & Repasi, E. (2015). *A TRM4 Component for the Night Vision Integrated Performance Model (NV-IPM)*. In G. C. Holst, & K. A. Krapels (Ed.), SPIE Defense + Security; Infrared Imaging Systems: Design, Analysis, Modeling, and Testing XXVI. Proc. of SPIE Vol. 9452. Baltimore: SPIE.

[16] Vollmerhausen, R. H., Jacobs, E., & Driggers, R. G. (2004, November). *New Metric for Predicting Target Acquisition Performance*. Optical Engineering, Optical Engineering 43 No. 11, 2806–2818.

[17] Teaney, B. P., Tomkinsno, D. M., & Hixson, J. G. (2015). *Legacy Modeling and Range Prediction Comparison: NV-IPM versus SSCamIP and NVTherm*. In G. C. Holst (Ed.), SPIE Defense + Security; Infrared Imaging Systems: Design, Analysis, Modeling, and Testing XXVI. Proc. of SPIE Vol. 9452. Baltimore: SPIE.

[18] Hixson, J. G., Jacobs, E. L., & Vollmerhausen, R. H. (2004). *Target Detection Cycle Criteria When Using the Targeting Task Performance Metric*. In R. G. Driggers, & D. A. Huckridge (Ed.), SPIE European Symposium on Optics and Photonics for Defense and Security; Electro-Optical and Infrared Systems: Technology and Applications. Proc. of SPIE Vol. 5612. London: SPIE.

[19] Night Vision Electronic Sensors Directorate (NVESD). (n.d.). *Night Vision - Integrated Performance Model (NV-IPM) TTP Metric 2006 Help*. Night Vision - Integrated Performance Model (NV-IPM), 1.11. NVESD.

[20] Boettcher, E., Leonard, K., Hodgkin, V. A., Hixson, J., Miller, B., Johnson, S., et al. (2010). *New Target Acquisition Task for Contemporary Operating Environments: Personnel in MWIR, LWIR, and SWIR*. In G. Holst, & K. A. Krapels (Ed.), SPIE

Defense, Security, and Sensing; Infrared Imaging Systems: Design, Analysis, Modeling, and Testing XXI. Proc. of SPIE Vol. 7662, 76620I. Orlando: SPIE.

APPENDIX A: Acronym List

Table 7: Acronym List

Acronym	Definition
AMOP	Average Modulation at Optimum Phase
CTF	Contrast Threshold Function
EDS	Effective Difference Signal
FOV	Field of View
GIQE	General Image Quality Equation
GRD	Ground Resolved Distance
GSD	Ground Sample Distance
GUI	Graphical User Interface
IFOV	Instantaneous Fields of Views
IIRS	Imagery Interpretability Rating Scale
JND	Just Noticeable Difference
MDSP	Minimum Difference Signal Perceived
MNDS	Minimum Necessary Difference Signal
MRC	Minimum Resolvable Contrast
MRT	Minimum Resolvable Temperature
MTF	Modulation Transfer Function
NIIRS	National Imagery Interpretation Rating System
NV-IPM	Night Vision – Integrated Performance Model
NVL	Night Vision Lab
OPD	Optical Path Difference
P(Task)	Probability of Task
PSF	Point Spread Function
RER	Relative Edge Response
RMS	Root Mean Squared
SNR	Signal to Noise Ratio
TRM	Thermal Range Model
TRM3	Thermal Range Model Version 3
TRM4	Thermal Range Model Version 4
TTP	Target Task Performance
TTPF	Target Task Performance Function
TTPM	Target Task Performance Metric
™	Trademark
USAF	United States Air Force
V-NIIRS	Video- National Imagery Interpretation Rating System

APPENDIX B: NIIRS Ratings

Table 8: NIIRS Definitions

(from [3, 8, 9, 10, 11])

Rating Level	Infrared Definition	Visible Definition	Civil Definition	Video Definition
0	• Interpretability of the imagery is precluded by obscuration, degradation, or very poor resolution	• Interpretability of the imagery is precluded by obscuration, degradation, or very poor resolution	• Interpretability of the imagery is precluded by obscuration, degradation, or very poor resolution	• Not Applicable
1	• Distinguish between runways and taxiways on the basis of size, configuration, or pattern at a large airfield • Detect a large clear in a dense forest (> 1 km^2) • Detect large ocean going vessels in open water • Detect large areas of marsh or swamp (> 1 km^2)	• Detect a medium-sized port facility and/or distinguish between taxi-ways and runways at a large airfield	• Distinguish between major land use classes (e.g., urban, forest, etc.) • Detect a medium-sized port facility • Distinguish between runways and taxiways at a large airfield • Identify large area drainage patterns by type (dendritic, trellis, etc.)	• Not Applicable
2	• Detect large aircraft • Detect individual large buildings in an urban area • Distinguish between densely wooded, sparsely wooded, and open field • Distinguish between naval and commercial port facilities based on type and configuration of large functional areas	• Detect large hangars at airfields • Detect large static radars • Detect military training areas • Detect large buildings at a naval facility • Detect large buildings	• Identify large center-pivot irrigated fields during the growing season (> 160 acre) • Detect large buildings • Identify road patterns, like clover leafs, on major highway systems • Detect ice-breaker tracks • Detect the wake from a large ship (> 300')	• Not Applicable

Rating Level	Infrared Definition	Visible Definition	Civil Definition	Video Definition
3	• Distinguish between large and small aircraft • Identify individual thermally active flues running between the boiler hall and smoke stacks at a thermal power plant • Detect a large radar site based on the presence of mounds, revetments and security fencing • Detect a driver training track at a ground forces garrison • Distinguish between large freighters and tankers	• Identify the wing configuration (e.g., straight, swept, delta) of all large aircraft • Detect a helipad by the configuration and markings • Identify a large surface ship in port by type (e.g., cruiser, auxiliary ship, etc.) • Detect trains or strings of standard rolling stock on railroad tracks (not individual cars)	• Detect large area contour plowing (> 160 acre) • Detect individual houses in residential neighborhoods • Detect trains or strings of standard rolling stock on railroad tracks (not individual cars) • Identify inland waterways navigable by barges • Distinguish between natural forest stands and orchards	• Visually track the movement of missile transporter and support vehicles, making a turn, on improved roads
4	• Identify the wing configuration of small fighter aircraft • Detect a small electrical transformer yard in an urban area (~ 50 m^2) • Detect large environmental domes at an electronics facility (> 10 m dia.) • Detect individual thermally active vehicles in garrison • Identify individual closed cargo hold hatches on large merchant ships	• Identify all large fighters by type • Detect the presence of large individual radar antennas • Identify, by general type, tracked vehicles, field artillery, etc., wheeled vehicles when in groups • Identify individual tracks, rail pairs, control towers, switching points in rail yards	• Identify farm buildings as barns, silos, or residences • Count unoccupied railroad tracks along right-of-way or in a railroad yard • Detect basketball court, tennis court, volleyball court in urban areas • Identify individual tracks, rail pairs, control towers, switching points in rail yards • Detect jeep trails through grassland	• Visually track movement of tracked vehicles and trailers, making a turn during tactical road on an unpaved road
5	• Distinguish between single-tail and twin-tailed fighters • Identify outdoor tennis courts • Identify the metal lattice structure of large radio relay towers (~ 75 m) • Detect armored vehicles in a revetment	• Identify radar as vehicle-mounted or trailer-mounted • Identify individual rail cars by type (e.g., gondola, flat, box) and/or locomotives by type (e.g., steam, diesel)	• Identify Christmas tree plantations • Identify individual rail cars by type (e.g., gondola, flat, box) and locomotives by type (e.g., steam, diesel) • Detect open bay doors of vehicle storage buildings • Identify tents at established	• Visually confirm the rotation of the turret on a main battle tank

Rating Level	Infrared Definition	Visible Definition	Civil Definition	Video Definition
	• Identify the stack shape (e.g., square, round, oval) on large merchant ships (> 200 m)		recreational camping areas (> 2 person) • Distinguish between stands of coniferous and deciduous trees during leaf-off condition • Detect large animals (e.g., elephants, rhinoceros, giraffes) in grasslands	
6	• Detect wing-mounted stores protruding from the wings of large bombers • Identify individual thermally active engine vents atop diesel locomotives • Distinguish between thermally active tanks and Armored Personal Carriers (APCs)	• Distinguish between models of small/medium helicopters • Identify the spare tire on a medium-sized truck • Identify automobiles as sedans or station wagons	• Distinguish between row (e.g., corn, soybean) crops and small grain (e.g., wheat, oats) crops • Identify automobiles as sedans or station wagons • Identify individual telephone/electric poles in residential neighborhoods • Detect foot trails through barren areas	• Visually track the movement of an identified vehicle; car, SUV, van, pickup truck; driving independently on roadways in medium traffic
7	• Identify automobiles as sedans or station wagons • Identify antenna dishes on a radio relay tower (< 3 m dia.) • Detect mooring cleats or bollards on piers.	• Identify fitments and fairings on a fighter-sized aircraft • Identify ports, ladders, vents on electronics vans • Identify individual rail ties	• Identify individual mature cotton plants in a known cotton field • Identify individual railroad ties • Detect individual steps on a stairway • Detect stumps and rocks in forest clearings and meadows	• Visually confirm the movement of unidentified deck-borne objects as they are dumped over the side or stern of any surface ship or fishing vessel at sea
8	• Identify limbs (e.g., arms, legs) on an individual • Identify individual horizontal and vertical ribs on a radar antenna • Detect closed hatches on a tank turret • Identify individual posts and rails on deck edge life rails	• Identify the rivet lines on bomber aircraft • Detect winch cables on deck-mounted cranes • Identify windshield wipers on a vehicle	• Count individual baby pigs • Identify a USGS benchmark set in a paved surface • Identify grill detailing and/or the license plate on a passenger/truck type vehicle • Identify individual pine seedlings • Identify individual water lilies	• Visually confirm the movement of an individual holding a shoulder fired antiaircraft missile as the launcher is raised to the aimed firing position

Rating Level	Infrared Definition	Visible Definition	Civil Definition	Video Definition
			on a pond • Identify windshield wipers on a vehicle	
9	• Identify access panels on fighter aircraft • Identify cargo (e.g., shovels, rakes, ladders) in an open-bed, light-duty truck • Identify turret hatch hinges on armored vehicles • Identify individual rungs on bulkhead mounted ladders	• Differentiate cross-slot from single slot heads on aircraft skin panel fasteners • Identify vehicle registration numbers on trucks • Identify braid of ropes (1” to 3” dia.) • Detect individual spikes in railroad ties	• Identify individual grain heads on small grain (e.g., wheat, oats, barley) • Identify individual barbs on a barbed wire fence • Detect individual spikes in railroad ties • Identify individual bunches of pine needles • Identify an ear tag on large game animals (e.g., deer, elk moose)	• Visually confirm the movement of the body and limbs of an individual holding a long rifle as the weapon is raised to an aimed firing position -either standing, sitting, or prone
10	• Not Applicable	• Not Applicable	• Not Applicable	• Visually confirm the movement of the hands and forearms of an individual holding a compact assault weapon as the weapon is raised either standing, crouched, or prone
11	• Not Applicable	• Not Applicable	• Not Applicable	• Visually confirm the movement of individual's fingers and hands while aiming a shoulder fired anti-tank missile as they release safety and arm the device at a tactical position in a rural or urban environment

APPENDIX C: MATLAB Script

```
% Mark Burgener
% OPTI 909
% Master's Report

clear
clc
close all

%%

clear
clc
close all

% This section defines the N50 values for the original
Johnson Criteria.
D_N50 = 1.0;
O_N50 = 1.4;
R_N50 = 4.0;
I_N50 = 6.4;

n = 1;

% This for loop calculates the E and P(Task) values over a
given range.
for N = 0:0.1:30
    Ed(n) = 2.7+0.7*(N/D_N50);
    Eo(n) = 2.7+0.7*(N/O_N50);
    Er(n) = 2.7+0.7*(N/R_N50);
    Ei(n) = 2.7+0.7*(N/I_N50);

    P_d(n) = ((N/D_N50).^Ed)/(1+((N/D_N50).^Ed));
    P_o(n) = ((N/O_N50).^Eo)/(1+((N/O_N50).^Eo));
    P_r(n) = ((N/R_N50).^Er)/(1+((N/R_N50).^Er));
    P_i(n) = ((N/I_N50).^Ei)/(1+((N/I_N50).^Ei));

    n = n+1;
end

N1 = 0:0.1:30;
```

```
legendCell =
{'Detection','Orientation','Recognition','Identification'};

figure
plot(N1,P_d,'-k','LineWidth',1)
xlim([0 10])
ylim([0 1])
hold on
plot(N1,P_o,'--k','LineWidth',1)
plot(N1,P_r,':k','LineWidth',2)
plot(N1,P_i,'-.k','LineWidth',1)
hold off
title('A Comparison of Task Performance and Actual
Cycles');
xlabel('Number of Cycles');
ylabel('Probability of Task Performance');
legend(legendCell,'Location','southeast');

% This section defines the 2D N50 values for the original
Johnson Criteria.
D_2d_N50 = 0.75;
C_2d_N50 = 1.5;
R_2d_N50 = 3.0;
I_2d_N50 = 6.0;
E_high = 3.8;
E_casual = 1.73;
nn = 1;

% 2D Johnson for loop calculates the E and P(Task) values
over a given range.
for N = 0:0.1:30
    E_2dd(nn) = 1.75+0.35*(N/D_2d_N50);
    E_2dc(nn) = 1.75+0.35*(N/C_2d_N50);
    E_2dr(nn) = 1.75+0.35*(N/R_2d_N50);
    E_2di(nn) = 1.75+0.35*(N/I_2d_N50);

    P_2dd(nn) =
((N/D_2d_N50).^E_2dd)/(1+((N/D_2d_N50).^E_2dd));
    P_2dc(nn) =
((N/C_2d_N50).^E_2dc)/(1+((N/C_2d_N50).^E_2dc));
    P_2dr(nn) =
((N/R_2d_N50).^E_2dr)/(1+((N/R_2d_N50).^E_2dr));
```

```
    P_2di(nn) =
((N/I_2d_N50).^E_2di)/(1+((N/I_2d_N50).^E_2di));

    P_2di_fixedE_high(nn) =
((N/I_2d_N50).^E_high)/(1+((N/I_2d_N50).^E_high));
    P_2di_fixedE_casual(nn) =
((N/I_2d_N50).^E_casual)/(1+((N/I_2d_N50).^E_casual));

    nn = nn+1;
end

legendCell_1 =
{'Detection','Classification','Recognition','Identification
'};

figure
plot(N1,P_2dd,'-k','LineWidth',1)
xlim([0 10])
ylim([0 1])
hold on
plot(N1,P_2dc,'--k','LineWidth',1)
plot(N1,P_2dr,':k','LineWidth',2)
plot(N1,P_2di,'-.k','LineWidth',1)
hold off
title('A Comparison of 2D Task Performance and Actual
Cycles');
xlabel('Number of Cycles');
ylabel('Probability of Task Performance');
legend(legendCell_1,'Location','southeast');

legendCell_2 = {'1D Detection','2D Detection'};
legendCell_3 = {'Orientation','Classification'};
legendCell_4 = {'1D Recognition','2D Recognition'};
legendCell_5 = {'1D Identification','2D Identification'};
legendCell_6 = {'1D Identification','2D Identification','2D
Identification Fixed E High','2D Identification Fixed E
Casual'};


figure
plot(N1,P_d,'-k','LineWidth',1)
xlim([0 10])
ylim([0 1])
hold on
```

```
plot(N1,P_2dd,':k','LineWidth',2)
hold off
title('A Comparison of 1D and 2D Detection Task
Performance');
xlabel('Number of Cycles');
ylabel('Probability of Task Performance');
legend(legendCell_2,'Location','southeast');

figure
plot(N1,P_o,'-k','LineWidth',1)
xlim([0 10])
ylim([0 1])
hold on
plot(N1,P_2dc,':k','LineWidth',2)
hold off
title('A Comparison of 1D and 2D Orientation and
Classification Task Performance');
xlabel('Number of Cycles');
ylabel('Probability of Task Performance');
legend(legendCell_3,'Location','southeast');

figure
plot(N1,P_r,'-k','LineWidth',1)
xlim([0 10])
ylim([0 1])
hold on
plot(N1,P_2dr,':k','LineWidth',2)
hold off
title('A Comparison of 1D and 2D Recognition Task
Performance');
xlabel('Number of Cycles');
ylabel('Probability of Task Performance');
legend(legendCell_4,'Location','southeast');

figure
plot(N1,P_i,'-k','LineWidth',1)
xlim([0 10])
ylim([0 1])
hold on
plot(N1,P_2di,':k','LineWidth',2)
hold off
title('A Comparison of 1D and 2D Identification Task
Performance');
xlabel('Number of Cycles');
```

```
ylabel('Probability of Task Performance');
legend(legendCell_5,'Location','southeast');


%%

clear
clc
close all

% Treat a gray-scale image (maybe the one on the website)
as a sampled object f(x; y). Now,
% create 3 psf's of various resolutions. Plot profiles of
the psf's and the OTF's. Take your
% object through each imaging system. Make sure that one of
your OTF's has zeros in it after
% certain spatial frequencies.

% Reads in the image
img = imread('969px-USAF-1951.svg.png');
img = rgb2gray(img);
img = double(img);

Nx = 969;
Ny = 1024;

% Sets the sample spacing in the x direction.
x = linspace(-1,1,Nx+1);
x = x(1:Nx);

% Sets the sample spacing in the y direction.
y = linspace(-1,1,Ny+1);
y = y(1:Ny);

% Calculates the spacing in the Fourier domain.
delx = x(2)-x(1);
dely = y(2)-y(1);
xi = linspace(-1/(2*delx),1/(2*delx),Nx+1);
yi = linspace(-1/(2*dely),1/(2*dely),Ny+1);

% Creates the meshgrid for 2D plots.
[Y,X] = meshgrid(x,y);

% Sets R to define the Gaussian PSFs.
```

```
R = sqrt(X.^2+Y.^2);

% Generates the PFSs based on Office Hour recommendations
psf1 = exp(-10000000*R.^2);
psf2 = exp(-7500*R.^2);
psf3 = exp(-500*R.^2);

% Per Equation 3 in the lab the OTF is the FFT of the PSF.
This section
% calculates the OTFs based on the defined PSFs.
OTF1 = real(fftshift(fft2(fftshift(psf1))))*delx*dely;
OTF2 = real(fftshift(fft2(fftshift(psf2))))*delx*dely;
OTF3 = real(fftshift(fft2(fftshift(psf3))))*delx*dely;

MTF1 = abs(OTF1);
MTF2 = abs(OTF2);
MTF3 = abs(OTF3);

% This takes the FFT of the image so we can work in Fourier
space to get
% away from the convolution operator.
IMG = fftshift(fft2(fftshift(img)))*delx*dely;

% This is the implementation of Equation 5 to calculate the
Fourier domain
% version of the final image.
IMGF1 = OTF1.*IMG;
IMGF2 = OTF2.*IMG;
IMGF3 = OTF3.*IMG;

% This takes the IFFT of the blurred images to return a
spatial domain
% image.
imgf1 = real(fftshift(ifft2(fftshift(IMGF1))))*delx*dely;
imgf2 = real(fftshift(ifft2(fftshift(IMGF2))))*delx*dely;
imgf3 = real(fftshift(ifft2(fftshift(IMGF3))))*delx*dely;

% This section plots the images.
figure
subplot(2,2,1)
imagesc(img)
title('Original Image')
colormap(gray)
axis off ;
```

```
axis square;

subplot(2,2,2)
imagesc(imgf1)
title('Blurred Image with a Small PSF')
colormap(gray)
axis off ;
axis square;

subplot(2,2,3)
imagesc(imgf2)
title('Blurred Image with a Medium PSF')
colormap(gray)
axis off ;
axis square;

subplot(2,2,4)
imagesc(imgf3)
title('Blurred Image with a Large PSF')
colormap(gray)
axis off ;
axis square;

MTF11 = MTF1(1,:);
MTF11 = rescale(MTF11);
MTF21 = MTF2(1,:);
MTF21 = rescale(MTF21);
MTF31 = MTF3(1,:);
MTF31 = rescale(MTF31);

figure
plot(xi(486:969),MTF11(486:969))
%hold on

figure
plot(xi(486:969),MTF21(486:969))
%plot(xi(486:969),MTF31(486:969))
%hold off

figure
plot(xi(486:969),MTF31(486:969))

%%
```

```
clear
clc
close all

Freq = [0
0.008683468
0.017366936
0.026050404
0.034733872
0.04341734
0.052100808
0.060784276
0.069467744
0.078151212
0.08683468
0.095518149
0.104201617
0.112885085
0.121568553
0.130252021
0.138935489
0.147618957
0.156302425
0.164985893
0.173669361
0.182352829
0.191036297
0.199719765
0.208403233
0.217086701
0.225770169
0.234453637
0.243137105
0.251820573
0.260504041
0.26918751
0.277870978
0.286554446
0.295237914
0.303921382
0.31260485
0.321288318
0.329971786
```

0.338655254
0.347338722
0.35602219
0.364705658
0.373389126
0.382072594
0.390756062
0.39943953
0.408122998
0.416806466
0.425489934
0.434173402
0.442856871
0.451540339
0.460223807
0.468907275
0.477590743
0.486274211
0.494957679
0.503641147
0.512324615
0.521008083
0.529691551
0.538375019
0.547058487
0.555741955
0.564425423
0.573108891
0.581792359
0.590475827
0.599159295
0.607842763
0.616526231
0.6252097
0.633893168
0.642576636
0.651260104
0.659943572
0.66862704
0.677310508
0.685993976
0.694677444
0.703360912
0.71204438

0.720727848
0.729411316
0.738094784
0.746778252
0.75546172
0.764145188
0.772828656
0.781512124
0.790195592
0.798879061
0.807562529
0.816245997
0.824929465
0.833612933
0.842296401
0.850979869
0.859663337
0.868346805
0.877030273
0.885713741
0.894397209
0.903080677
0.911764145
0.920447613
0.929131081
0.937814549
0.946498017
0.955181485
0.963864953
0.972548422
0.98123189
0.989915358
0.998598826
1.007282294
1.015965762
1.02464923
1.033332698
1.042016166
1.050699634
1.059383102
1.06806657
1.076750038
1.085433506
1.094116974

1.102800442
1.11148391
1.120167378
1.128850846
1.137534314
1.146217782
1.154901251
1.163584719
1.172268187
1.180951655
1.189635123
1.198318591
1.207002059
1.215685527
1.224368995
1.233052463
1.241735931
1.250419399
1.259102867
1.267786335
1.276469803
1.285153271
1.293836739
1.302520207
1.311203675
1.319887143
1.328570612
1.33725408
1.345937548
1.354621016
1.363304484
1.371987952
1.38067142
1.389354888
1.398038356
1.406721824
1.415405292
1.42408876
1.432772228
1.441455696
1.450139164
1.458822632
1.4675061
1.476189568

1.484873036
1.493556504
1.502239973
1.510923441
1.519606909
1.528290377
1.536973845
1.545657313
1.554340781
1.563024249
1.571707717
1.580391185
1.589074653
1.597758121
1.606441589
1.615125057
1.623808525
1.632491993
1.641175461
1.649858929
1.658542397
1.667225865
1.675909333
1.684592802
1.69327627
1.701959738
1.710643206
1.719326674
1.728010142
1.73669361
1.745377078
1.754060546
1.762744014
1.771427482
1.78011095
1.788794418
1.797477886
1.806161354
1.814844822
1.82352829
1.832211758
1.840895226
1.849578694
1.858262163

```
1.866945631
1.875629099
1.884312567
1.892996035
1.901679503
1.910362971
1.919046439
1.927729907
1.936413375
1.945096843
1.953780311
1.962463779
1.971147247
1.979830715
1.988514183
1.997197651
2.005881119
2.014564587
2.023248055
2.031931524
2.040614992
2.04929846
2.057981928
2.066665396
];

Amp = [1.345987153
0.016118734
0.008403722
0.005857028
0.004600897
0.003861729
0.003381967
0.003050523
0.002812072
0.002636111
0.002504591
0.002405527
0.002331303
0.002276993
0.002238232
0.002210042
0.002190972
0.002181085
```

0.002183736
0.002196887
0.002216437
0.002242122
0.002273144
0.002309573
0.002351174
0.002397288
0.002448072
0.002503705
0.002563909
0.00262841
0.002697514
0.002770955
0.002849049
0.002931505
0.003018685
0.003111559
0.003219574
0.003333403
0.003453432
0.003579128
0.003711004
0.003848797
0.003993906
0.004145548
0.004304039
0.004469544
0.004643518
0.004824383
0.005013132
0.005210888
0.00541644
0.005631105
0.005855286
0.006100682
0.006366692
0.006643278
0.006934041
0.007237309
0.007555017
0.007887284
0.008234548
0.008598431

0.00897829
0.009376565
0.009792319
0.010228197
0.010683682
0.011160494
0.011659896
0.012182654
0.012739742
0.013347802
0.013993619
0.014670094
0.015382736
0.016133952
0.016919881
0.017755377
0.018627927
0.019556074
0.020528984
0.021554377
0.022641172
0.023787313
0.024994514
0.026279837
0.027621515
0.029061535
0.030621517
0.032291067
0.03407434
0.035974673
0.03796567
0.040126535
0.042399233
0.04482515
0.047417841
0.050195604
0.0531098
0.056382342
0.059871246
0.063619725
0.067906507
0.07284599
0.07806554
0.083751085

0.090013561
0.096808658
0.103995482
0.112033217
0.120626243
0.130003872
0.139998839
0.151291432
0.163272346
0.176437358
0.190661785
0.206652614
0.22363847
0.2424515
0.262960032
0.286038754
0.310896559
0.337782327
0.367481186
0.400970099
0.436830323
0.477020453
0.521276033
0.571652627
0.625963793
0.687338576
0.754896524
0.832976978
0.917858048
1.014745372
1.121056272
1.2466893
1.384706487
1.544233992
1.718681768
1.915702181
2.136975809
2.394381084
2.680842362
3.016830093
3.405079358
3.864255751
4.38445004
5.006376314

5.72401032
6.610875125
7.640871217
8.908844457
10.40431108
12.29848845
14.63367806
17.66096094
20.91530749
25.13659749
30.39202865
37.46338921
46.54341701
59.10655882
76.0333736
100.9524453
137.5905757
197.1175963
294.4821092
482.3275003
868.4221781
1950.355543
5474.4326
12464.51892
6404.791886
2387.08627
1250.453652
812.1913899
577.5198129
436.3701962
345.4397498
282.4859076
237.7463819
204.9249504
179.9603839
160.1417748
144.4121312
131.4764012
120.9630825
112.5481578
105.4953505
99.43158221
94.44807378
92.36377176

90.52250585
89.31237415
88.29209858
87.45073844
86.73797232
86.19715484
85.76500932
85.7228486
85.94836936
86.31320893
86.73379034
87.30268173
87.92160685
88.70067106
89.94510518
91.36112588
93.86994649
97.16805135
100.5633744
104.1885064
107.9887015
112.5875888
117.3388533
122.4304927
127.7112154
133.402204
139.3290398
145.8000818
153.3524273
161.5466736
170.1587293
179.5626259
189.5030377
200.7440373
215.5248308
232.6285088
251.7147894
272.715099
295.9764636
321.7497653
350.5941478
382.8096328
419.9540643
463.8196343

```
514.2860407
];

T = zeros(239,1);
T(1:1:end) = 3.11;

N = 1.172;

x = [0.7 0.775];
y = [0.6 0.5];
S = linspace(10^-4,T(146),10);
S1 = zeros(size(S));
S1(1:end) = Freq(146);

figure
h = semilogy(Freq,Amp,'k',Freq,T,':k',S1,S,'--
k',Freq(146),T(146),'sk','MarkerFaceColor','k')
xlim([0 1.5])
set(h(1),'LineWidth',1);
set(h(2),'LineWidth',2);
set(h(3),'LineWidth',1);
annotation('textarrow',x,y,'String','Cut of Frequency')
title('Example of N Linked to System CTF');
xlabel('Frequency');
ylabel('Amplitude');
legend('System CTF','Apparent Target Contrast')
```